BILINGUAL PUBLISHING CO.
Pioneer of Global Academics Since 1984

Journal of Building Material Science

Volume 4 • Issue 2 • December 2022 ISSN 2630-5216(Online)

BILINGUAL PUBLISHING CO.
Pioneer of Global Academics Since 1984

Volume 4 Issue 2 • December 2022 • ISSN 2630-5216 (Online)

JOURNAL OF BUILDING MATERIAL SCIENCE

BILINGUAL PUBLISHING CO.
Pioneer of Global Academics Since 1984

BILINGUAL PUBLISHING CO.
Pioneer of Global Academics Since 1984

Volume 4 | Issue 2 | December 2022 | Page1-45
Journal of Building Material Science

Contents

Articles

BILINGUAL PUBLISHING CO.
Pioneer of Global Academics Since 1984

Journal of Building Material Science
https://ojs.bilpublishing.com/index.php/jbms

ARTICLE

Properties of Sawdust Concrete

Onyechere, Ignatius Chigozie*

Department of Civil Engineering, Federal University of Technology, Owerri, Nigeria

ARTICLE INFO

Article history
Received: 23 June 2022
Revised: 6 September 2022
Accepted: 13 September 2022
Published Online: 29 September 2022

Keywords:
Sawdust ash
Pozzolan
Concrete
Ordinary Portland Cement
Compressive strength

ABSTRACT

This work examined the structural properties of concrete obtained by partially replacing cement with sawdust ash. The sawdust ash which is a pozzolan was obtained by burning sawdust which is a waste product from processing of timber in an open air. The burnt ash was passed through a 150 μm metric sieve to obtain the ash used. Physical and chemical analysis were performed on the ash to verify its suitability as a partial substitute for cement in concrete. Chemical analysis was also carried out on the Ordinary Portland Cement (OPC) sample. Concrete mixes were produced by replacing OPC with 0%, 5%, 10%, 20% and 30% of Sawdust Ash (SDA). Both fresh and hardened properties of the concrete produced were investigated. The chemical investigation on the ash showed that it contained most of the basic compounds found in OPC making it suitable to serve as a partial substitute for OPC in concrete. Investigation on the concrete showed that both the workability and density of the concrete reduce as the SDA content increases. Analysis on the hardened concrete revealed that the compressive strength of the concrete decreases as the ash content increases for the early ages of curing. However, from 21 days curing age upwards, the compressive strength decreases as SDA increases up to 10% of SDA at which the compressive strength rose to a maximum value, and then starts reducing again as the percentage SDA increases. Thus, the SDA concrete gained rapid strength at later ages indicating its pozzolanic activity.

1. Introduction

Concrete is a composite inert material that is mainly made up of a binding agent (e.g. lime, ordinary Portland cement, pozzolans, etc.), mineral filler or aggregates and water. Sometimes an additional material known as admixture is added to modify certain properties of the concrete [1]. Before the advent of the portland cement, clay and lime-based materials were some of the traditional binders used by man in the production of concrete and mortar for building construction [2].

The important features of both the fresh and hardened concrete include workability, compressive strength, rate of setting and hardening, deformation under load, durability, permeability, shrinkage, etc. However, compressive strength is considered to be an important property and the

*Corresponding Author:
Onyechere, Ignatius Chigozie,
Department of Civil Engineering, Federal University of Technology, Owerri, Nigeria;
Email: onyecherechigozie@gmail.com

DOI: https://doi.org/10.30564/jbms.v4i2.4818

quality of concrete is often judged by its strength.

It is a well-known fact cement is the most expensive constituent of concrete, which makes the overall cost of concrete to be too high. Shetty and Jain [3] affirmed that in 1996, the global production of cement was estimated at about 1.3 billion tons, for each ton produced, 0.87 tons of CO_2 was expelled, thus, 7% of the world's emission of CO_2 is attributed to Portland cement production.

Hence, because of the high cost of cement, its significant contribution to environmental pollution and the high consumption of natural resources such as limestone, we cannot go on producing more and more cement. This justifies the search for a more environmentally friendly and less expensive binding agent to substitute cement in concrete. In the past, such searches for alternative cement led to the discovery of pozzolans. A pozzolan is a natural or artificial material that contains silica or a combination of silica and aluminium which has little or no cementitious value but when in finely divided form and also in the presence of water, it will chemically react with lime (produced during the hydration of Portland cement) at ordinary temperatures to yield compounds that possess cementitious properties [4]. According to Neville and Brooks [5], concrete produced from a mixture of Portland cement and pozzolan will gain strength slowly and hence, needs to be cured for a comparatively long period of time, but the long-term strength is high. Pozzolan or Pozzolana needs to be in finely divided form so as to present a larger surface area to the alkali solutions for the reaction to take place [6].

In the recent times, the ash from many agricultural wastes in Nigeria have been found to possess pozzolanic characteristics and are thus used as supplementary cement in concrete [7]. The use of these wastes as concrete materials promotes sustainability in the production of structural concrete [7].

Several researchers have worked on the use of various agricultural waste in concrete. Siddique, Singh, Mehta and Belarbi [8] used varying percentages of water and sodium silicate treated sawdust to replace sand in concrete and observed that, concrete produced from 5% water and sodium silicate treated sawdust yielded compressive strength approximately of the same magnitude with that of the control concrete. In the works of Alabduljabbar, Huseien, Sam, Alyouef, Algaifi and Alaskar [9], sawdust was used to replace fine/coarse aggregate incorporating fly ash and granulated blast furnace slag to produce high-performance light weight concrete without cement. It was observed from their work that the thermal conductivity coefficient, the workability, density, setting time and compressive strength of the concrete decreases with increase in sawdust content while the general acoustic properties of the concrete was enhanced as revealed by the increase in noise reduction and sound absorption coefficients of the concrete with increase in sawdust content. Farnaz Batool, Kamrul Islam, Celal Cakiroglu, and Anjuman Shahriar [10] produced concrete in which the fine aggregate was partially replaced with untreated sawdust. In their work, they reported that the micrographs from their works showed a wider formation of cracks and interface gaps in the cement matrix, these gaps and cracks were however, found to contract after immersing the concrete in sulphate for a period of 28 days which also improved the compressive strength. Hassen and Hameed [11] studied the properties of sawdust cement mortar treated with Hypochlorite and observed that there was an improvement in the compressive strength and reduction in dry density with increase in washed and treated sawdust content in the mixture. El-Nadoury [12] investigated the properties of concrete produced by partially replacing sand and cement in concrete with sawdust and sawdust ash respectively. Ettu, Osadebe and Mbajiorgu [13] partially replaced Ordinary Portland Cement (OPC) with ash from eight different agricultural wastes such as Rice Husk, Cassava peels, Cocoanut shells, Paw-paw leaf, Plantain leaf, Corn cob, Sawdust and Oil palm bunch. In their work, they observed that the compressive strength of the concrete produced increased with increase in curing age and decreased with increase in percentage replacement of OPC with each ash. Parande, Stalin, Thangarajan, and Karthikeyan [14] used a mixture of rice husk ash, bagasse ash, fly ash and bye product from thermal waste to partially replace cement in concrete from 5% to 30%. In their work, they observed that as the percentage replacement level increased, the water absorption of the concrete increased. Patel M., Patel K., Patel A., Prajapati and Koshti [15] used sawdust as fine aggregate to partially replace sand in concrete. In their work, they increased the percentage replacement of sharp sand with sawdust gradually from 0-30%, the compressive and split tensile strength of the concrete produced decreases with increase in percentage replacement with sawdust.

Elinwa [16] used a mixture of Gum Arabic and Sawdust Ash to replace cement in concrete and discovered that with the Gum Arabic alone, the mechanical strength of the concrete increased, but with the mixture of Gum Arabic and Sawdust Ash, the mechanical strength of the concrete decreased. It was observed in the works of Elinwa and Abdukadir [17] that when SDA is used in reinforced concrete, it delays the process of corrosion of the reinforcements.

Sawdust is the loose particles of wood produced as waste products during the processes of sawing and converting timber into different sizes and shapes [18]. These particles are burnt to ashes to produced sawdust ash. Apart

from reducing the cost of concrete, use of pozzolanas such as sawdust ash, an agricultural waste material promotes waste management at little cost as waste is being converted into money, and also solves the problem of environmental pollution created by these wastes.

2. Materials and Methods

The materials for the concrete used in this study are ordinary Portland cement (Dangote 3X Brand), aggregates (fine and coarse), Sawdust ash and water.

The ordinary Portland cement used in this study has physical and chemical properties that complies with the requirements of the British Standards [19].

The coarse aggregate used in this study was crushed granite having maximum size of 20 mm. The aggregate was sourced from a granite quarry at Ishiagu in Ebonyi State, Nigeria. It has a gray colouration, an irregular shape and a rough surface texture.

The fine aggregate used in this work was sand obtained from Otamiri River which is the major source of sharp sand for Owerri and its environs. From the grain size distribution analysis carried out on the sand, it complies with the specifications of BS.882 [20] for fine aggregates. The sand was dry and free from deleterious materials.

Sawdust Ash used in this work was obtained by burning sawdust (which is wood shavings and dust obtained as waste during the various stages of processing of timber) in an open air to ashes. The ash used in this work is the particles of the ash that passed through the 150 mm standard sieve size. The sawdust was obtained from a timber sawmill situated at the wood market at Naze in Owerri, Imo State, Nigeria. The sawdust was obtained from various local wood varieties. The local wood varieties used are Mahogany, Ubia, Gmelina, Rubber, Akwammiri, Ebelebe Udele, Udah, Imieghu and Oweh.

Methodology

After burning the sawdust to ash, the ash obtained was sieved using British standard sieve of 150 mm diameter. The sawdust ash (SDA) sample used in this work was the ash materials that passed through the 150 mm sieve. The SDA sample was characterised by taking it to the laboratory to determine its physical and chemical properties. This was done by mixing the sample with water to form a cake-like texture. The briquettes were moulded according to the prescribed test i.e. porosity test, shrinkage test, rupture and plasticity test. The briquettes were coded, dried and fired to the desired temperature. Readings were taken after drying and firing to calculate the final results for the physical analysis. The OPC sample used was equally taken to the laboratory to determine its chemical composition. Sieve analysis was carried out on both the coarse and fine aggregates using the British standard sieves to determine the grain size distribution of the aggregates. The following parameters were deducted from the results of the sieve analysis:

$$Coefficient\ of\ Uniformity,\ C_u = \frac{D_{60}}{D_{10}}, \tag{1}$$

$$Coefficient\ of\ Curvature,\ C_c = \frac{{D_{30}}^2}{D_{10}.\ D_{60}} \tag{2}$$

Dxx is the particle size corresponding to xx percentage passing [21].

The test specimen for compressive strength is a concrete cube of size; 150 mm × 150 mm × 150 mm as recommended by BS 1881: Part 116 [22]. A concrete mix ratio of 1:2.58:3.42 and a water-cement ratio of 0.57 was used in producing concrete cube specimens. The batching of concrete was done by mass and a total of five different batches were made. For each of the five different batches, OPC was replaced with 0%, 5%, 10%, 20% and 30% by mass of SDA respectively. Slump test was carried out on each concrete mix to determine its workability. After a period of twenty-four (24) hours of casting, the concrete cubes produced were cured by totally submerging them in a water tank. For each percentage replacement of OPC with SDA, two cubes each were cast and cured for a period of 7, 14, 21 and 28 days respectively. After curing, the cube was brought out of water and left to dry after a little period of time and weighed on a weighing balance to determine its self-weight. Thereafter, the cube was taken to a universal testing machine having a maximum capacity of 1000 kN and was placed with the cast faces placed in contact with the platens of the crushing machine and the value of the load in kN at which a cube fails during crushing is recorded. The compressive strength and the density of the cube are obtained from the following equations:

$$\text{Compressive Strenrth} = \frac{\text{Failure Load}}{150 \text{ x } 150} \left(N/_{mm^2}\right) \tag{3}$$

$$\text{Density} = \frac{\text{Self Weight}}{0.15\text{x}0.15 \text{ x } 0.15} \left(kg/_{m^3}\right) \tag{4}$$

3. Results and Discussions

3.1 Physical and Chemical Properties of Sawdust Ash

The results of the physical and chemical properties of the SDA were presented on Tables 1 and 2 respectively. Table 3 shows a comparison between the chemical composition of the SDA and that of the OPC.

Table 1. Summary of the Physical Properties of SDA

S/N	Parameter	Value
1	Porosity	85.40%
2	Water Absorption	74.59%
3	Apparent Density	1.146
4	Bulk Density	8.03
5	Shrinkage	3.6%
6	Modulus of Plasticity	3.32
7	Making Moisture	29.547%
8	Modulus of Rupture	1.172 kg/cm^2
9	Loss on Ignition	61.00

Table 2. Summary of the Chemical Composition of SDA

S/N	Oxide	Percentage by Mass (%)
1	SiO_2	20.8
2	CaO	3.22
3	Al_2O_3	1.53
4	Fe_2O_3	3.58
5	Na_2O	0.20
6	K_2O	0.22
7	PbO	0.02
8	MgO	5.14
9	MnO	0.008
10	LOI	61.0
	Total	95.718

Table 3. Comparisons between the Chemical Compositions of SDA and OPC

S/N	Compound	Percentage by Mass	
		SDA	OPC
1	SiO_2	20.80	21.20
2	CaO	3.22	64.73
3	Al_2O_3	1.53	5.02
4	Fe_2O_3	3.58	3.08
5	Na_2O	0.20	0.19
6	K_2O	0.22	0.42
7	MgO	5.14	1.04
8	MnO	0.01	-
9	PbO	0.02	-
10	SO_3	-	2.01
11	LOI	61.00	1.45
	Others	4.282	0.66

From Table 1, the SDA has high water absorption (74.59%), this is as a result of its high porosity of 85.4%. The making moisture of the SDA is high (29.55%) and this is as a result of its high porosity. The chemical composition of SDA in Table 2 showed that the total sum of Fe_2O_3, SiO_2 and Al_2O_3 is 25.91%. This value is far below the required value of 70% minimum for pozzolanas [4]. Table 1 shows that the Loss on Ignition of the SDA is 61.0%. This is far above the 12% maximum required for pozzolanas [4]. This shows that the ash used contained much unburnt carbon which reduces its pozzolanic activity. This shortcoming of the SDA used might have resulted from the improper method of combustion through which the ash was obtained.

Table 3 shows that there is great similarity between the chemical composition of the SDA and that of OPC and hence, SDA can to a reasonable extent serve as an alternative cement.

3.2 Results on Grain Size Distribution.

The sieve analysis results of the coarse and fine aggregates are presented in Table 4, Figure 1, and Table 5, Figure 2 respectively.

Table 4. Sieve Analysis Result for Coarse Aggregates

Sieve Size (mm)	Mass Retained	Cummulative Mass Retained	% Cummulative Mass Retained	% Passing
37.50	0.00	0.00	0.00	100.00
19.00	11.20	11.20	1.13	98.87
14.00	448.98	460.18	46.26	53.74
10.00	456.70	916.88	92.18	7.82
5.60	77.60	994.48	99.98	0.02
3.35	0.20	994.68	100.00	0.00
Receiver	285.02			

$$D_{10} = 10.1899,\ \ D_{30} = 11.9321, D_{60} = 14.6936 \quad (5)$$

$$C_u = 1.442\ ,\ \ C_c = 0.951 \quad (6)$$

Table 5. Sieve Analysis Result for Fine Aggregates

Sieve Size (mm)	Mass Retained (g)	Cummulative Mass Retained (g)	% Cummulative Mass Retained	% Passing
10.000	0.00	0.0	0.00	100.00
5.600	1.90	1.9	0.38	99.62
3.350	7.80	9.7	1.94	98.06
2.000	45.80	55.5	11.12	88.88
1.180	94.00	149.5	29.95	70.05
0.600	129.50	279.0	55.89	44.11
0.425	125.00	404.0	80.93	19.07
0.300	47.20	451.2	90.38	9.62
0.212	30.50	481.7	96.49	3.51
0.150	13.50	495.2	99.20	0.80
0.063	4.00	499.2	100.00	0.00
Receiver	279.80			

$$D_{10} = 0.305,\ \ D_{30} = 0.5014, D_{60} = 0.9553 \quad (7)$$

$$C_u = 3.1321\ ,\ \ C_c = 0.8628 \quad (8)$$

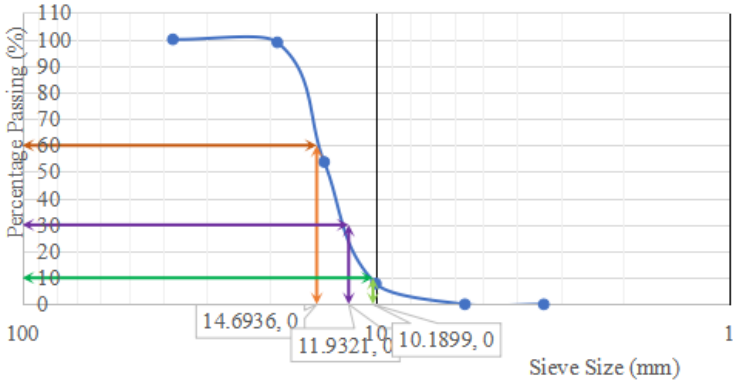

Figure 1. Sieve Analysis for Coarse Aggregates

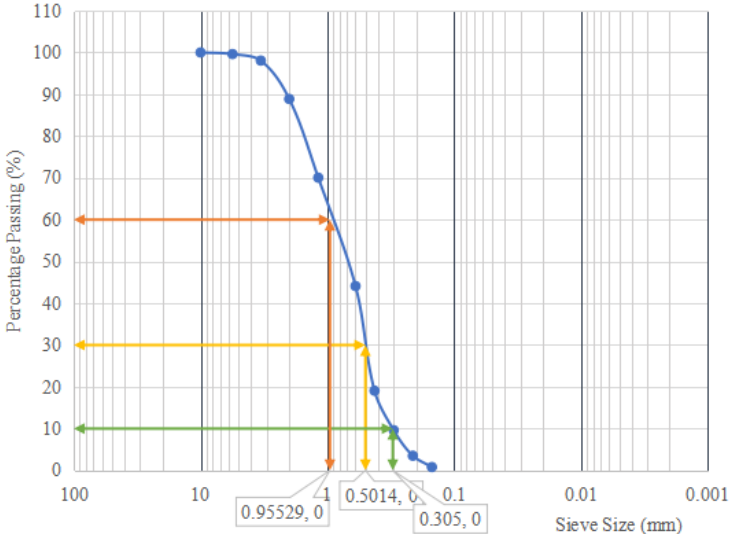

Figure 2. Sieve Analysis for Fine Aggregates

From Tables 4 and 5 and Figures 1 and 2, using the Unified Soil Classification System (USCS), since for the fine aggregate, $C_u < 6$ *and* $C_c < 1$, the fine aggregate is classified as "Poorly Graded Sand". Also, for the coarse aggregates, $C_u < 4$ *and* $C_c < 1$, the coarse aggregate is classified as "Poorly Graded Gravel".

3.3 Workability of Fresh Concrete

The results of the slump tests on the fresh concrete mixes are presented in Table 6 and Figure 3.

Table 6. Workability of concrete with SDA

SDA %	Slump (mm)
0	80
5	75
10	70
20	25
30	20

The slump test results of the SDA/OPC concrete mixes given in Table 6 and Figure 3, show a decrease in the workability of the concrete as the SDA content increases.

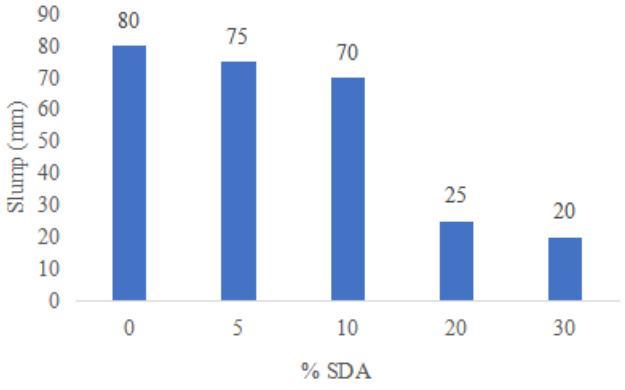

Figure 3. Slump Test Result

3.4 Compressive Strength of the Concrete

The compressive strength results of Equation (3) and dry density results of Equation (4) for the various mixes

at different curing ages are presented on Tables 7, 8, 9, 10 and 11. The variation of the compressive strength of the concrete mixes with different SDA content at various curing ages is presented in Figures 4 and 5.

Table 7. Compressive Strength Result at 7 days of Curing

%SDA		Wt. of cube (kg)	Density (kg/m^3)	Average Density (kg/m^3)	Crushing Load (kN)	Strength (N/mm^2)	Average Length (N/mm^2)
0	1	8.30	2459	2489	490.00	21.8	24.0
	2	8.50	2519		590.00	26.2	
5	1	8.20	2430	2415	511.00	22.7	20.7
	2	8.10	2400		420.00	18.7	
10	1	8.10	2400	2408	349.00	15.5	16.3
	2	8.1`5	2415		382.00	17.0	
20	1	8.20	2430	2400	284.00	12.6	12.6
	2	8.00	2370		282.00	12.5	
30	1	8.10	2400	2378	192.00	8.5	9.2
	2	7.95	2356		222.00	9.9	

Table 8. Compressive Strength Result at 14 days of Curing

%SDA		Wt. of cube (kg)	Density (kg/m^3)	Average Density (kg/m^3)	Crushing Load (kN)	Strength (N/mm^2)	Average Length (N/mm^2)
0	1	8.40	2489	2460	590.00	26.2	26.0
	2	8.20	2430		580.00	25.8	
5	1	8.30	2459	2430	563.00	25.0	24.6
	2	8.10	2400		545.00	24.2	
10	1	8.30	2459	2408	653.00	29.0	25.0
	2	7.95	2356		470.00	20.9	
20	1	8.05	2385	2393	462.00	20.5	21.0
	2	8.10	2400		482.00	21.4	
30	1	8.00	2370	2385	442.00	19.6	19.6
	2	8.10	2400		440.00	19.6	

Table 9. Compressive Strength Result at 21 days of Curing

%SDA		Wt. of cube (kg)	Density (kg/m^3)	Average Density (kg/m^3)	Crushing Load (kN)	Strength (N/mm^2)	Average Length (N/mm^2)
0	1	8.35	2474	2437	594.00	26.4	26.3
	2	8.10	2400		590.00	26.2	
5	1	8.40	2489	2430	592.00	26.3	25.7
	2	8.00	2370		565.00	25.1	
10	1	8.25	2444	2422	646.00	28.7	28.6
	2	8.10	2400		640.00	28.4	
20	1	8.05	2385	2378	620.00	27.6	25.2
	2	8.00	2370		514.00	22.8	
30	1	7.94	2353	2377	490.00	21.8	21.7
	2	8.10	2400		485.00	21.6	

Table 10. Compressive Strength Result at 28 days of Curing

%SDA		Wt. of cube (kg)	Density (kg/m^3)	Average Density (kg/m^3)	Crushing Load (kN)	Strength (N/mm^2)	Average Length (N/mm^2)
0	1	8.40	2489	2467	596.00	26.5	26.9
	2	8.25	2444		614.00	27.3	
5	1	8.30	2459	2459	592.00	26.3	26.6
	2	8.30	2459		605.00	26.9	
10	1	8.25	2444	2437	650.00	28.9	29.4
	2	8.20	2430		670.00	29.8	
20	1	8.15	2415	2421	572.00	25.4	25.3
	2	8.19	2427		564.00	25.1	
30	1	8.18	2424	2408	470.00	20.9	22.9
	2	8.07	2391		558.00	24.8	

Table 11. Compressive Strength Result for concrete mixes with SDA.

% SDA	Compressive Strength (N/mm^2)			
	7 Days	14 Days	21 Days	28 Days
0	24.0	26.0	26.3	26.9
5	20.7	24.6	25.7	26.6
10	16.3	25.0	28.6	29.4
20	12.6	21.0	25.2	25.3
30	9.2	19.6	21.7	22.9

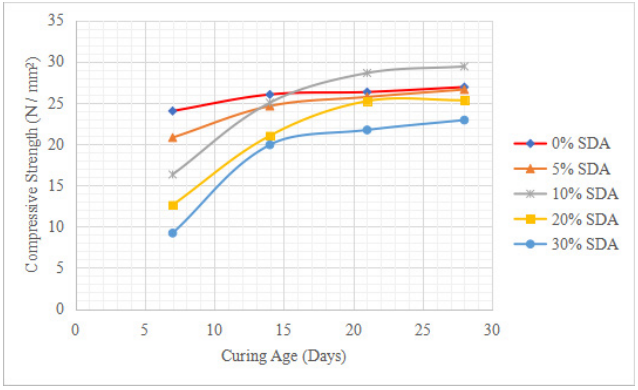

Figure 4. Variation of the Compressive Strength of Concrete mixes at various curing ages.

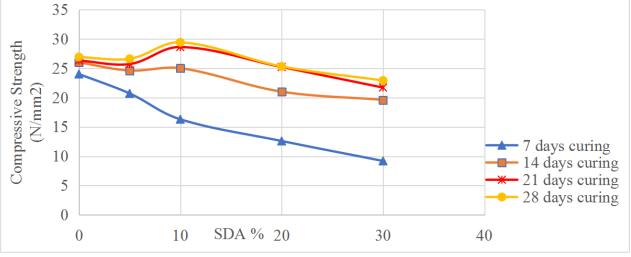

Figure 5. Variation of the Compressive Strength of Concrete mixes at different percentages of SDA.

Figures 4 and 5, and Table 11 show that for all the percentages of SDA content in the concrete, the compressive strength of the concrete increases as the curing age increases. Also Figure 4 shows that, from 16 days of curing upwards, the compressive strength of the concrete with 10% SDA became higher than that of the 0%, 5%, 20% and 30% SDA content in concrete. Figure 5 showed that at 10% SDA content in concrete and 28 days curing age, the compressive strength of the concrete assumed the highest value of 29.4 N/mm^2 which is higher than that of the control mix (the mix with 0% SDA or 100% cement) whose value is 26.9 N/mm^2. Also after 10% SDA content, the compressive strength decreases as the percentage SDA in the concrete increases. Tables 7, 8, 9 and 10 show that the dry density of the SDA/OPC concrete decreases as the percentage replacement of SDA increases. This indicates that the SDA is of lighter weight than the OPC.

4. Conclusions

The Sawdust ash under study has similar chemical compounds that are found in OPC but in varied quantities. SDA has a high water absorption, low plasticity and a high porosity.

The SDA/OPC concrete assumes higher strength at longer age of curing. At 10% replacement of cement with SDA, the highest compressive strength of 29.4 N/mm^2 was achieved at 28 days of curing, thus, 10% SDA in concrete yields optimum result. Above this percentage

(10%), the compressive strength of the concrete decreases.

Though there are some similarities between the physical and chemical properties of SDA and that of OPC, however, SDA has high porosity, high shrinkage, low modulus of rupture, low SiO_2, Al_2O_3 and CaO content and hence, is not suitable for total replacement but rather, partial replacement of cement in concrete.

By using SDA to partially replace cement which is the most expensive constituent of concrete in Nigeria, the entire cost of concrete construction is thus, reduced.

Recommendations

Concrete construction industries should incorporate SDA in their mix so as to save cost and reduce the environmental pollution otherwise caused by sawdust.

Partial replacement of cement with 10% SDA in concrete is recommended for structural concrete while higher percentage up to 30% of SDA in concrete is recommended for light load bearing structures.

It is recommended that incinerators be used in burning sawdust so as to ensure complete combustion to ash to enhance its pozzolanic capacity.

Author Contributions

The entire work was solely authored by Ignatius Chigozie Onyechere.

Funding

This research received no external funding.

Acknowledgments

I specially acknowledge the contributions of Engr. Prof. Augustine Uchechukwu Elinwa of the department of Civil Engineering, Abubakar Tafawa Balewa University, Bauchi, Nigeria. He inspired to carry out this research.

Conflict of Interest

There is no conflict of interest.

References

[1] Surahyo, A., 2019. Concrete Construction: Practical Problems and Solutions, 2nd ed.; Springer Nature: Switzerland. pp. 1-320.

[2] Heinemann, H.A., Nijland, T.G., 2016. Historic Lime-Binders: An Example of 19th Century Dutch Military Plain Concrete. Materials and Environment (CiTG), Delft University of Technology, The Netherlands. https://www.researchgate.net/publication/289550096.

[3] Shetty, M.S., Jain, A.K., 2019. Concrete Technology: Theory and Practice; S. Chand Publishing, New Delhi. pp. 1-350.

[4] ASTM C618-06: Standard Specification for Coal Fly Ash and Raw or Calcined Natural Pozzolan for Use in Concrete. Annual Book of ASTM standards. American Society for Testing and Materials Vol. 04-02.

[5] Neville, A.N., Brooks, J.J., 2010. Concrete Technology, 2nd ed., Pearson Education Limited: England. pp. 1-442.

[6] Newman, J., Choo, B.S., 2003. Advanced Concrete Technology; Constituent Materials, Elsevier Ltd: Great Britain.

[7] Fapohunda, C., Kilani, A., Adigo, B., et al., 2021. A Review of Some Agricultural Wastes in Nigeria for Sustainability in the Production of Structural Concrete. Nigerian Journal of Technological Development. 18(2), 76-87.

[8] Siddique, R., Singh, M., Mehta, S., et al., 2020. Utilization of treated saw dust in concrete as partial replacement of natural sand. Journal of Cleaner Production. 261(10).
DOI: https://doi.org/10.1016/j.jclepro.2020.121226

[9] Alabduljabbar, H., Huseien, G.F., Sam, A.R.M., et al., 2020. Engineering Properties of Waste Sawdust-Based Lightweight Alkali-Activated Concrete: Experimental Assessment and Numerical Prediction. Materials. 13(5490), 1-30.
DOI: https://doi.org/10.3390/ma13235490

[10] Batool, F., Islam, K., Cakiroglu, C., et al., 2021. Effectiveness of Wood Waste Sawdust to Produce Medium- to Low-Strength Concrete Materials. Journal of Building Engineering. 44.
DOI: https://doi.org/10.1016/j.jobe.2021.103237

[11] Hassen, S.A., Hameed, S.A., 2020. Physical and Mechanical Properties of Sawdust Cement Mortar Treated with Hypochlorite. IOP Conference Series: Materials Science and Engineering. 745, 012149.
DOI: https://doi.org/10.1088/1757-899X/745/1/012149

[12] El-Nadoury, W.W., 2021. Production of Sustainable Concrete Using Sawdust. Magazine of Civil Engineering. 105(5).
DOI: https://doi.org/10.34910/MCE.105.7

[13] Ettu, L.O., Osadebe, N.N., Mbajiorgu, M.S.W., 2013. Suitability of Nigerian Agricultural By-Products as Cement Replacement for Concrete Making. International Journal of Modern Engineering Research (IJMER). 3(2), 1180-1185.

[14] Parande, A.K., Stalin, K., Thangarajan, R.K., et al., 2011. Utilization of Agroresidual Waste in Effective Blending in Portland Cement. International Scholarly

Research Network. 2011.
DOI: https://doi.org/10.5402/2011/701862

[15] Patel, M., Patel, K., Patel, A., et al., 2016. Study of Sawdust Concrete Properties as Construction Materials. 3rd International Conference on Multidisciplinary Research & Practice. IV(1), 201-205.

[16] Elinwa, A.U., 2021. Mechanical Strengths of Sawdust-Ash-Admixed Gum Arabic Concrete. Journal of Modern Materials. 8(1), 12-29.
DOI: https://doi.org/10.21467/jmm.8.1.12-29

[17] Elinwa, A.U., Abdulkadir, S., 2016. Sawdust Ash as an Inhibitor for Reinforcement Corrosion in Concrete. MOJ Civil Engineering. 1(3), 1-5.
DOI: https://doi.org/10.15406/mojce.2016.01.00015

[18] Okoroafor, S.U., Ibearugbulam, O.M., Onukwugha, E.R., et al., 2017. Structural Characteristics of Sawdust-Sand-Cement Composite. International Journal of Advancements in Research & Technology. 6(1), 173-180.

[19] BS EN 197-1:2000. Cement: Composition, Specifications and Conformity Criteria for Common Cements. British Standards Institution, London.

[20] BS 882, 1992. Specifications for Aggregates from Natural Sources for Concrete. British Standards Institution, London.

[21] Frata, D., Aguettant, J., Roussel-Smith, L., 2007. Soil Mechanics Laboratory Testing. CRC Press, Taylor & Francis Group: New York.

[22] Jackson, N., Dhir, K.R., 1996. Civil Engineering Materials, 5th ed. Palgrave, China. pp. 106 - 126.

BILINGUAL PUBLISHING CO.
Pioneer of Global Academics Since 1984

Journal of Building Material Science
https://ojs.bilpublishing.com/index.php/jbms

ARTICLE

Heating, Ventilation and Air Conditioning Design for Commercial Complex Buildings: Theory and Method Based on Inverse Problem

Yu Zhang*

Building Design Institute, China Academy of Building Research, Beijing, 100013, China

ARTICLE INFO

Article history
Received: 19 October 2022
Revised: 9 November 2022
Accepted: 1 December 2022
Published Online: 3 December 2022

Keywords:
Science and technology
Design optimization

ABSTRACT

Scientific and technological progress and innovation help the design industry, which plays an important role in sustainable development. It will improve the operation efficiency of enterprises and explore a blue sea for enterprise. In essence, design should be the process of deriving the optimal scheme from different schemes or imaginary scenes. Based on this, this paper proposes an overall optimization method for Heating, Ventilation and Air Conditioning (HVAC) design. Compared with the traditional design method, under certain constraints, it can obtain the optimal design scheme that maximizes the value of the designed product. This study provides new inverse problem ideas and methods for HVAC designers, and provides solutions for enhancing the value of HVAC design products.

1. Introduction

Since the outbreak of the epidemic in 2020, the development of enterprises has also been affected. At the same time, with the continuous development of society, the internal and external competition between enterprises is also constantly sublimated. This is both an opportunity and a challenge for most enterprises. The progress of science and technology provides more opportunities for the development of modern enterprises, and also puts forward higher standards for the quality of enterprises' products. Therefore, strengthening the exploration and guidance of scientific and technological innovation and optimizing the product structure of enterprises have played a crucial role in the development of enterprises.

The energy consumption of building operation is about one third of the commercial energy of the whole society. China is in the high-speed stage of economic development, which has continued the rapid growth of GDP for more than ten years, and the annual growth rate of energy consumption is also high. As a pillar industry of GDP growth, the construction industry's annual total construction volume is close to half of the global annual total construction volume. Building energy consumption increases with the increase of the total number of buildings. Whether China can achieve sustainable development is not only closely related to the improvement of people's quality of life, but also related to the implementation of national en-

*Corresponding Author:
Yu Zhang,
Building Design Institute, China Academy of Building Research, Beijing, 100013, China;
Email: sdjyzhq@163.com

DOI: https://doi.org/10.30564/jbms.v4i2.5167

ergy strategy and resource conservation strategy, as well as global climate change and sustainable development.

At present, China's building energy consumption (excluding rural non commodity biomass energy) has been maintained at 20% ~ 25% of the total social energy consumption and is increasing. From 2000 to 2010, the energy consumption for construction and operation increased from 289 million tons of standard coal to 677 million tons of standard coal. From 2030 to 2040, China's population will reach a peak of 1.47 billion, and the urbanization rate will reach 70%. Under this background, the urban residential and industrial building areas will further increase. Some scholars pointed out that in the future, China's total building volume will reach 91 billion square meters, which is twice the current total building volume, which will also increase the energy consumption brought by buildings. The International Energy Agency (IEA) predicts that by 2030, China's total energy consumption will reach 5.81 billion tons of standard coal, including 1.52 billion tons of standard coal for building energy consumption.

In 2018, China's carbon emissions reached 9.8 billion tons, accounting for about 28.8% of the world's total. The total carbon emissions from building operation and construction are about 2.35 billion tons, accounting for 24% of the national carbon emissions, and the building materials are about 1.65 billion tons, accounting for 16%, accounting for 5% of the global total carbon emissions.

Therefore, research on building energy conservation is not only an important way to achieve energy conservation and emission reduction in China, but also related to the sustainable development of global energy and environment.

HVAC energy consumption is a large part of building operation energy consumption, and due to the complexity and large size of HVAC equipment, the HVAC system will also affect the building scheme. On the one hand, the refined HVAC design method can effectively reduce the energy consumption of the HVAC system. With the help of optimization design, the energy consumption problem in the later period can be solved in the early stage to save energy consumption. On the other hand, the building layout can be reasonably used to improve the use value of the building.

The traditional HVAC design concept is generally to solve the direct problems: know the building envelope information, climate conditions and indoor personnel, the heating of lights and equipment and ventilation times, and the layout of machine room shafts, calculate the cooling and heating loads of buildings and the selection and layout of air conditioning and ventilation equipment. The limitations of the current design concepts include that the designers cannot know which enclosure structure can reduce the heating and air conditioning load as much as possible on the premise of meeting the indoor thermal comfort. It is impossible to know the ideal natural ventilation strategy and heating and air conditioning strategy. It is impossible to know the ideal HVAC room and shaft layout. The current design concepts are to solve the direct problems, not optimization. In order to solve the shortage of traditional design concepts, this paper proposes that HVAC design should solve the inverse problem. The objectives of this work are: (1) to put forward an approach for determining the ideal HVAC room and shaft layout. (2) to demonstrate the advantage of applying the approach in practice by using some illustrative examples.

2. Research Problem

In general, the traditional HVAC design is to solve direct problems (as shown in Figure 1). The reason and effect of this design idea are as follows: under the limited design conditions of building materials, designers cannot know what kind of thermal properties of building envelope materials can reduce heating and air-conditioning loads as much as possible. The optimal natural ventilation strategy cannot be determined. The minimum energy consumption of heating and air conditioning cannot be determined. The ideal positions of HVAC machine rooms and shafts cannot be known.

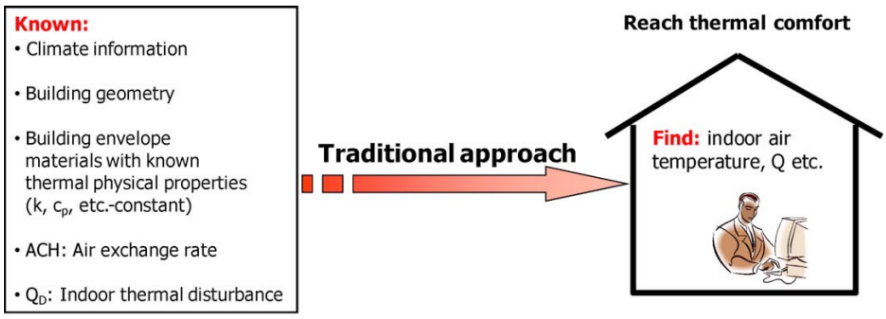

Figure 1. Traditional HVAC design ideas

This research attempts to apply the idea of inverse problem to HVAC design. Contrary to the traditional idea, this research idea takes thermal comfort requirements, load requirements, effective use area requirements, customer experience requirements, etc. as known quantities, and takes the thermal properties of the enclosure structure and the machine room shaft (including location, area, responsible area, and internal equipment air volume) as unknown quantities to solve (as shown in Figure 2) [1].

Because the parameters to be solved are functions, this kind of inverse HVAC problem is a nonlinear problem, which brings some difficulties to the solution. Because every inversion calculation in the inverse problem needs to solve the forward problem, the whole solving process is very tedious, so the large amount of calculation is another difficulty in solving the inverse problem.

2.1 Inverse Problem Introduction

Julia, a famous American mathematician described the inverse problem as follows: "Usually in mathematics, you will get an equation, and you need its solution. Now you have a solution, and you must find that equation. I am happy to do so." The inverse problem is relative to the positive problem. In the process of understanding the world, human beings always receive various signals according to their sense organs to explore the development laws of objective things. On the basis of understanding the development law of objective things, people can calculate the unknown parameters from the known parameters according to the law. The signal is called external cause, the relationship becomes internal cause (the difference between external cause and internal cause is that there is a changing temporal relationship between the former and the structure, while the latter does not). Finding the result from the cause (external cause and internal cause) is called a direct problem, and finding the cause from the result (external cause or internal cause) is called an inverse problem.

Generally, we will give the cause signal (such as initial condition, boundary condition, etc.) according to the theory and practical experience of predecessors, and then carry out gradual reasoning to get the results. But in practical engineering, the initial conditions and boundary conditions can not be completely determined sometimes. At this time, it is necessary to inverse solve the uncertain factors in the system through some information obtained in time and space.

The formulation of the inverse problem originated in the 1960s, and then rapidly developed into a new cross discipline, which is widely used in natural science and engineering practice [2-4]. For example, seismic exploration, whose mechanism is that the seismic wave generated by the ground explosion propagates downward and reflects to the ground, judges the distribution of the underground medium through the vibration data received by the sensor. In the process of spacecraft returning, due to aerodynamic heating, the surface heat flow density is extremely high, but its accurate value cannot be directly measured, so the inverse heat conduction problem can be solved to determine its surface heat flow. For vibration flaw detection, the ultrasonic signal generator is used to generate sound pressure, and the fault is judged according to the reflected echo captured by the ultrasonic detector due to encountering cracks. The problem of heart death is to diagnose heart disease through inversion of cardiac electric field. The principle of CT technology is to transmit some physical quantities (such as various rays, particles, waves, electromagnetic fields, etc.) that can pass through the object without damaging the structure of the object, and then analyze the received signals of these physical quantities to obtain the object structure. Through calculation and processing, a three-dimensional perspective image of the internal structure of the object is established. Although inverse problems are widely used in physics, chemistry, aerospace, biology and other engineering disciplines, they can still be classified from different perspectives [5,6].

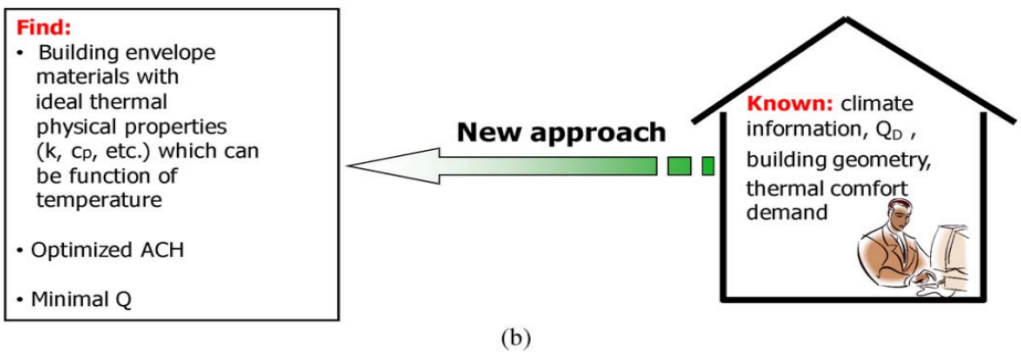

Figure 2. New ideas for HVAC design

The inverse problem has the following three characteristics:

(1) Non linearity: Judge the linearity and nonlinearity of the parameter to be solved according to its position in the model, and the nonlinearity is universal. Most inverse problems are nonlinear, and many inverse problems corresponding to linear positive problems are nonlinear, which brings some difficulties to solve inverse problems.

(2) Inadequate: Due to the error of observation, the solution to the rhetorical question does not exist or is not unique, which is the characteristic of ill posed. This is the difficulty of inverse problem research and application.

(3) Large amount of calculation: Every iteration of variables in the inverse problem requires recalculation of the positive problem, which makes the whole inversion process very cumbersome and consumes a lot of calculation time.

2.2 Inverse Problem Solving Method

Because of the nonlinearity, ill-posedness and large amount of computation, it is difficult to solve the inverse problem. In order to overcome these difficulties, researchers have developed many methods to solve inverse problems, which can be divided into three categories:

(1) Analytic and semi analytical methods: starting from the analytical formula of the forward problem, find the integral equation that connects the known conditions with the inverse problem, and then use mathematical tools (such as integral transformation) to solve the integral equation. Analytic method can use various mathematical skills to solve specific inverse problems with specific mathematical methods. The advantages of this method are: low calculation cost. The disadvantage is that it is only applicable to some simple linear problems.

(2) Non heuristic inversion algorithm: search the whole model space according to certain constraints, calculate all these models forward in turn, compare the calculation results with the measured data, and select the appropriate model. Typical non heuristic inversion algorithms include simulated annealing, genetic algorithm, etc. This method has the advantages of strong global convergence and the disadvantages of many iterations.

(3) Heuristic inversion algorithm: the idea is to form an iterative format for nonlinear problems, and gradually approximate to solve inversion variables. The basic principle is to start from an initial model, search near the initial model according to a certain method, obtain the model correction amount, and modify the original model according to the correction amount to obtain a new model. Repeat until convergence is satisfied. Including: steepest descent method, conjugate gradient method, sequential quadratic programming method, etc. The advantages of this method are: fast convergence speed, small amount of calculation, and the disadvantages are: the global convergence is not perfect.

Based on the characteristics of HVAC design, sequential quadratic programming (SQP) is used to solve this kind of inverse problem. Sequential quadratic programming is a feasible direction method. This algorithm can be regarded as a generalization of unconstrained descent algorithm. The strategy is to start from the feasible point and search along the descending feasible direction to find a new feasible point that makes the objective function value descend. The main step of the algorithm is to select the search direction and the step size to move along this direction. The idea of sequential quadratic programming method is to transform the constrained optimization problem into an unconstrained optimization problem by modifying the original problem, and then use Newton's method. In each iteration, the Hessian matrix of the Lagrangian function is approximated by the quasi Newton method, which produces a quadratic programming problem and ensures the convergence of each problem. The solution of the problem is used to determine the search direction, and the step size of each iteration is determined by linear search. SQP method includes three steps: updating Hessian matrix of Lagrangian function, solving quadratic programming problem, linear search and benefit function calculation.

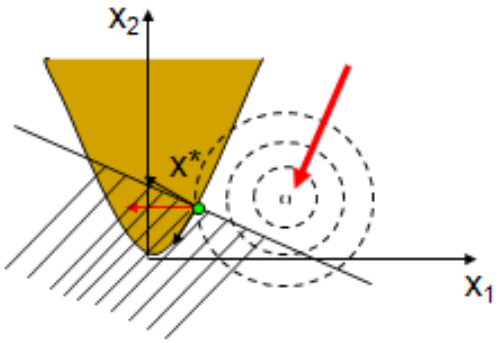

Figure 3. SQP categories

3. Results and Analysis

In order to reflect the advantages of applying the new HVAC design method to practical projects, this paper selects a commercial project in Beijing as an example for design. The project is a commercial complex building, with a total floor area of about 174688.45 m^2. There are three floors underground, and the total building area of the basement is about 60688.45 m^2. Business type: the first floor underground is equipment room, garage and non motor garage. The second underground floor is equipment

room, garage, non motorized garage, property room, etc. The third underground floor is garage, non motorized garage, etc. Thirteen floors above the ground, with a total floor area of about 114000 m^2 (including 74145 m^2 for commercial buildings), and the first to fifth floors are for commerce, cinemas and children's entertainment. Office on the sixth to thirteenth floors. The building height is about 59.95 m.

Taking the second floor as an example, the lower right corner of this floor area is a commercial business, requiring air supply by air conditioning units. The design constraints are: there are three fire compartments in this area, and the system setting does not allow crossing the fire compartment. No more than one group of air conditioning rooms in a group of fire compartments. The area of the air conditioner room shall A_e not exceed 50 m^2. The radius of the responsible area of the air conditioning machine room L not exceed 30 m. The air volume of the unit in the air conditioning room V not exceed 50000 m^3/h. The design variables are the location X and size S of the machine room, the responsible area and the unit air volume V_{ef} in the machine room. The design goal is to make the commercial effective leasable area A_{ef} as sufficient as possible.

After quantifying the above optimization problems, the optimization model can be obtained as follows:

Optimization objective: max A_{ef} (X, S, V_{ef})

Restrictive condition: $A_e \leq 50$; $L \leq 30$; $V \leq 50000$

Then, the numerical model is used to solve this problem. According to the grid independence test, it is found that the appropriate grid size of the air conditioning room is 100 mm.

Absolute error of the commercial effective leasable area between the numerical model and the analytical model is 6% at three different conditions. Therefore, the numerical model in this paper is acceptable.

After SQP method is adopted for calculation, the location map of the second floor air-conditioning room can be obtained (as shown in the black boxes in different color filled areas in Figure 4).

In order to verify the rationality of optimization, this paper compares the commercial effective rentable area under several different machine room locations, and finds that the optimized location of air-conditioning machine room can make the commercial effective rentable area the most sufficient.

The commercial effective leasable area has increased by 13% after optimization when air conditioning room is evenly distributed in the commercial complex building. The commercial effective leasable area has increased by 20% compared to air conditioning room concentrating on a fire compartment. The commercial effective leasable area has increased by 26% after optimization compared to air conditioning room distributed by unprinciple. This shows that the HVAC design method in this paper has advantages and operability in improving design quality and value.

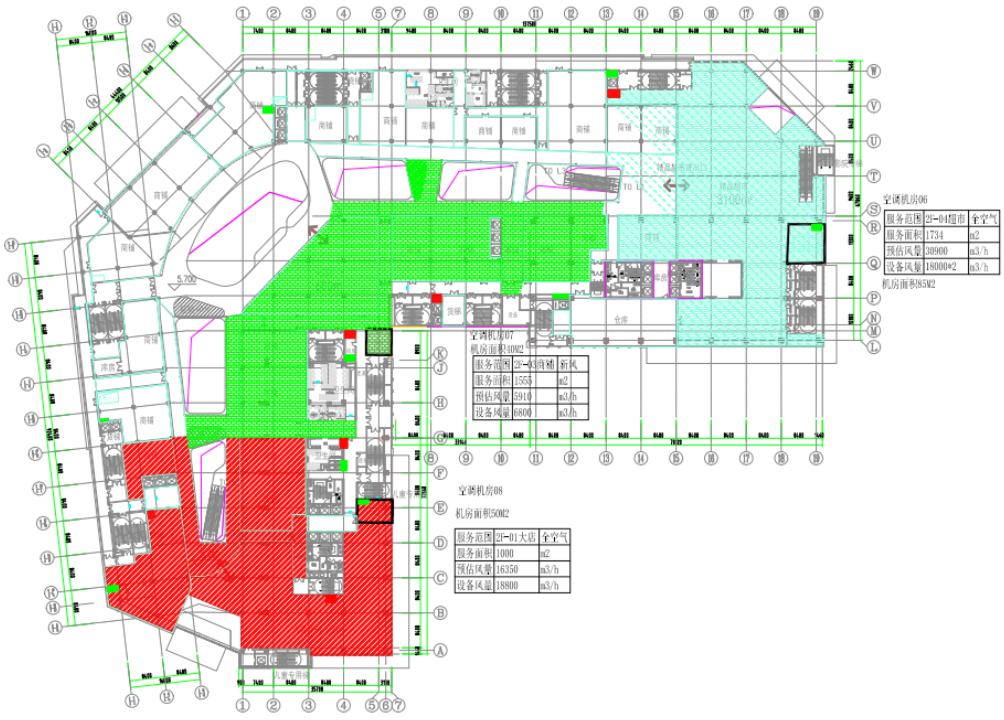

Figure 4. Layout plan of air-conditioning room on the second floor

4. Conclusions

(1) An approach of determining the ideal air-conditioning machine room distribution is put forward, which can realize the sufficient commercial effective leasable area.

(2) The result for a commercial project in Beijing as an example shows the optimal air-conditioning machine room distribution approaches a center distribution.

(3) The developed approach can also be used in the complex commercial for the purpose of designing.

This approach gives the guidelines for buildings' design in different regions to realize the energy conservation.

Conflict of Interest

There is no conflict of interest.

References

[1] Qadir, G., Haddad, M., Hamdan, D., 2019. Potential of energy efficiency for a traditional Emirati house by Estidama Pearl Rating system. Energy Procedia. (160), 707-714.

[2] Saxena, R., Rakshit, D., Kaushik, S.C., 2019. Phase change material (PCM) incorporated bricks for energy conservation in composite climate: A sustainable building solution. Solar Energy. (183), 276-284.

[3] Albayyaa, H., Hagare, D., Saha, S., 2019. Energy conservation in residential buildings by incorporating Passive Solar and Energy Efficiency Design Strategies and higher thermal mass. Energy and Buildings. (182), 205-213.

[4] Balli, L., Hlimi, M., Achenani, Y., et al., 2022. Experimental study and numerical modeling of the thermal behavior of an industrial prototype ceramic furnace: energy and environmental optimization. Energy and Built Environment.

[5] Ammaria, C., Belatracheb, D., Touhamic, B., et al., 2022. Sizing, optimization, control and energy management of hybrid renewable energy system—A review. Energy and Built Environment. (3), 399-411.

[6] Zhang, Y., Zhang, X., 2021. New Approach and Alternate Criterion for Heat-transfer Analysis of Building. Journal of Building Material Science. (03), 19-26.

BILINGUAL PUBLISHING CO.
Pioneer of Global Academics Since 1984

Journal of Building Material Science
https://ojs.bilpublishing.com/index.php/jbms

ARTICLE

Effect of Quartz Particle Size and Cement Replacement on Portland Limestone Cement Properties

Kachallah Bukar Gubio Muhammad Mukhtar Ismail Olubajo Olumide Olu*

Chemical Engineering Department, Abubakar Tafawa Balewa University, Bauchi, Bauchi State, 740102, Nigeria

ARTICLE INFO

Article history
Received: 23 September 2022
Revised: 9 November 2022
Accepted: 14 November 2022
Published Online: 17 November 2022

Keywords:
Quartz powder
Particle size
Consistence
Setting times
Mortar compressive strength

ABSTRACT

This research focuses on investigating the effect of quartz particle size and cement replacement on their physicomechnical properties. Portland limestone cement (PLC) was employed and replaced with quartz powder (QP) at various particle sizes (1.19 mm, 425 µm, 300 µm, 212 µm, <212 µm) and cement replacement between 2.5 wt.% ~ 15 wt.% at interval of 2.5 wt.% to study their impact on the cement properties. The PLC chemical composition revealed a relatively low lime and high silica content compared to the conventional cement. QP revealed a high silica, lime and sulphur contents compared to natural sand. A high consistence, elongated setting times and lower strengths and specific gravities were observed as cement was replaced with QP at a given particle size respectively. The effect of replacing cement with QP content between 2.5 wt.% and 15 wt.% at various particle sizes resulted in average increments by 45.32%, 23.13% and 36.06% for initial setting time, final setting time and water demand respectively. This increase could be related with clinker diminution coupled with enhanced QP surface area and clinker diminution. Similarly, an increase in the QP surface area at a given cement replacement led to higher water consistence, retarded setting times and lower strength. The effect of enhancing the QP' surface area between 1.19 mm and below 212 µm at a given cement replacement resulted in average increments by 26.27%, 8.61% and 7.49% for initial and final setting times and water demand respectively. The strength gain of the QP cement blend diminished significantly above 30% up to 15 wt.% cement replacement especially beyond 3 days. The low strength could be due to the high-water consistence linked with silica content resulting in setting time retardation. The optimal QP content was determined at 5 wt.% owing to the fact that the physicomechnical properties did not significantly deviate from the properties of control.

1. Introduction

Quartz powder is considered a natural and industrial byproduct obtained from mining activities such as sawing stones which can be employed as filler [1]; fine aggregate replacement and possess high void filling capacity which produces enhanced strength due to its high silicon content [2]. The QP is employed in the manufacture of both high and

*Corresponding Author:
Olubajo Olumide Olu,
Chemical Engineering Department, Abubakar Tafawa Balewa University, Bauchi, Bauchi State, 740102, Nigeria;
Email: ooolubajo@atbu.edu.ng

DOI: https://doi.org/10.30564/jbms.v4i2.5091

ultra-high-performance concrete and can be considered as chemically inert at room temperature, whereas at high temperature and pH [3,4]. They also possess relatively low hydraulic effect on cement [5]. The high purity quartzes are relevant in high technological industries such as semiconductors, high temperature lamp tubing, tele-communications, optics, microelectronics and solar silicon applications [6,7]. It is the second most abundant mineral on the earth surface after Feldspar and possesses a hardness of 7, white in color with a specific gravity between 2.6 and 2.7 [8]. It is a widely distributed mineral of many varieties which consist mainly of silica and other minor constituents including lithium, sodium, potassium and titanium having many applications ranging from glass manufacturing, ceramics, refractory materials. Crushed quartz could be used as an abrasive material for sand paper, etc. [9]. The decline in the natural resources encountered by the fast industrialization and urbanization of developing countries such as Nigeria coupled with the enormous demand for cement and sand in the construction sector, since is a serious concern. The increase in mining activities, enormous byproducts such as quartz resulting in waste generation. Thus, there is need to recycle these materials as cement replacement materials considered a promising prospect and could drive sustainability in the construction sector [10]. One solution to this menace is the use of these materials as either cement or fine aggregate replacement materials [11].

Finely ground quartz and limestone are mostly referred to as non-pozzolanic inorganic materials and may be considered a pozzolan despite exhibiting filler effect. The filler effect works on the principle of filling the voids in the cement matrix, thereby densifying the cement matrix resulting in acceleration of the early age hydration rate [12-18]. The provision of nucleation sites is responsible for the growth of more CSH and hydrates [19-20]. The use of finely ground quartz particle may either possess pozzolanic activity or filler effect is dependent on the particle size and surface area [21]. According to Yao *et al*. [22], investigated the effect of prolonged grinding (particle size) on the pozzolanic activity and hydration properties of quartz and suggested that the prolonged grinding led to a higher pozzolanic activity index, higher percentage alkaline dissolution in solution and lower crystallinity. Kadri *et al*. [23] observed that quartz with diameter between 20 µm and 25 µm did not exhibit pozzolanic activity and was considered a filler. The inclusion of fillers as one of the drivers for sustainability in the cement industry could provide economic, ecological and technical benefits as a result formation of more CSH despite clinker diminution [24-28].

Nikdel [52] investigated the effect of replacing cement with silica fume and observed its impact on the fresh and hardened states of concretes and was considered as an additive which could be employed as a cement replacement material. It was also believed that Portland cement mortars possesses a lot of voids, thus resulting in high permeability and low durability whereas if Portland cement was blended with QP, could fill up the voids and provide an enhanced permeability. Soumya & Karthiga [2] investigated the influence of replacing cement with silica fumes and fine aggregate with quartz on the concrete strength and found the optimal replacement to be 15%, 15% and 60% for concrete compressive, tensile and flexural strengths increments of 19.16%, 7.2% and 6.64% in comparison with 28 days control strengths respectively. Lin *et al*. [5] also studied the effect of water-binder ratio and quartz content on the properties of quartz-cement paste ranging from 0.2 and 0.5 and cement replacement ranging from 0%, 10% and 20% respectively. Results indicated that QP produced a dilution effect as well as a crystal nucleation effect on cement hydration which did not affect the hydration products monitored using XRF, XRD and SEM and TG techniques. Research findings suggested QP as chemically inert at room temperature whereas at elevated temperature and high pH, may not be inert [52]. It is also knowledge that inert fillers could enhance the degree of cement hydration by production of more nucleation site for C-S-H despite the fact that it could results in cement dilution [13]. There is a need to utilize the enormous waste materials being generated as a cement replacement has been tremendously employed owing to environmental, economic and technical benefits [29-31]. Arroudi *et al*. [32] investigated the effect of replacing cement with fine quartz from 15% to 25% on the fresh and mortar properties and observed that the presence of quartz did not influence the initial setting time but delayed the final setting time. The diminution of the clinker content by replacement of quartz results in decrease in the temperature rise leading to production of more CSH due to secondary hydration. The crystal structure of quartz is a significant factor in its pozzolanicity.

Tikkanen [33] investigated the effect of replacing cement between 10% and 40% at interval of 10% with quartz and it was observed that its concrete' compressive strength experienced increments beyond 7 and 28 days as well as the hydration kinetics were influenced. Popek & Sadowski [34,35] and Popek *et al*. [36] made attempts on several replacement materials such as quartz and quartz-feldspar mixture and basalts obtained from mining sites and concluded that the cement replacement with these materials significantly affect the mechanical properties owing to factors ranging from its quality to the amount of cement replaced. According to Ahmed *et al*. [37] observed that a high compressive strength was obtained at 20 wt.% crushed QP as a partial

replacement of fine sand and its strength gain was attributed to quartz being a good filler material whereas beyond 20 wt.% resulted in a reduction in its strength. Similarly, Galiska & Czarnecki [38] investigated beyond 30% cement replacement i.e., 40%-60% with quartz and quartz-feldspar powders affected the mechanical properties like tensile and compressive strength and was shown that the concrete compressive strength diminished by 6%-93% and 40%-65% of 7 days control compressive and tensile strength and diminished by 10%-85% and 17%-58% of the 28 days control compressive and tensile strength respectively as quartz content was increased. In conclusion, the strength of cement replaced with greater than 40% quartz-feldspar and quartz diminished significantly while the tensile strength was not negatively affected in comparison with control concrete for 7 and 28 days.

QP inclusion improved the concrete properties by physically acting as a filler and densifying and homogenizing the paste due to its fine particles, while surface chemical effect, is if the particle enhances hydration by acting as a part of the paste and increase in its surface area. The chemical effect by acting as a pozzolan to produce CSH [39]. Similarly, its inclusion in cement could also lead to Alkali Silica Reaction which is a major menace in many structures which occurs between silica and alkalis present in cement pastes in water saturated environment to produce amorphous silica gel that reacts with water and could result in expansion due to reaction, thus, deterioration of concrete's surface. Another unwanted phenomenon is carbonation in which calcium hydroxide produced from cement hydration reacts with CO_2 and affects the surface of concrete resulting in cracks for which one solution to this problem is the use of pozzolans. Thus, this paper tries to investigate the effect of replacing PLC with QP on the physico-mechanical properties such as consistence, initial and final setting time, soundness and mortar compressive strength as well as the effect of particle size on the cement properties.

2. Materials and Method

The quartz samples were collected at quarry site in Yelwa, Bauchi state and then sorted to remove unwanted materials, followed by size reduction into four main classes namely < 212 µm sieve, between 212 µm ~ 300 µm, between 300 µm ~ 425 µm and > 425 µm respectively. The particles that do not pass the sieve were recycled by grinding before being re-sieved. The QP sample required to obtain the chemical composition was ground to 75 µm and PLC CEM II A-L 42.5R were characterized via X-ray fluorescence spectrometer to obtain their chemical compositions.

The standard consistence and setting time tests were conducted and placed in a mold according to IS 4031 part 4 and 5 [40,41]/ASTM C 191 [42]. The experimental mix for the consistence and setting time of the various cement blends and control are presented in Table 1. The consistence and setting times of QP cement blends as well as PLC (control) were determined using a Vicat apparatus. This is achieved by addition of water at various percentage level until the paste indicates resistance to penetration. The penetration of the plunger into the paste should be between 5 mm ~ 7 mm above the bottom of the mould according to ASTM C 187 [43]. The consistence was recorded and obtained by arithmetic mean of three repetition and used in determining the setting times. The period elapsed between the time when the water was added to the cement and the time at which the needle ceased to descend beyond 4 mm from the bottom of the test block was noted as the initial setting time. In the case of the final setting time, the needle used for the initial setting time was replaced by a needle with annular attachment. The values of the initial and final setting times were determined by averaging three tests.

The mortar compressive strength of cement blend was conducted according to ASTM C 109 standard [44]. After proper mixing the mortar, the mix was transferred into the 50 mm cube moulds and compacted using a standard jolting apparatus and kept in a cabinet for 24 hours. The moulds were then demoulded and placed in curing tank containing water until the strength testing for 3, 7, 28 and 60 days. The experimental matrix for the determination of the physical and mechanical properties of PLC and QP cement blends are presented in Table 1.

Table 1. Experimental matrix for QP cement blend physicomechnical properties

S/No	Cement Blends	PLC %	QP %
1	PLC	100	0.0
2	2.5QP	97.5	2.5
3	5QP	95.0	5.0
4	7.5QP	92.5	7.5
5	10QP	90.0	10.0
6	12.5QP	87.5	12.5
7	15QP	85.0	15.0

3. Results and Discussion

The characterization of the QP, sand and PLC CEM II A-L 42.5R were carried out in Ashaka cement Plc to determine the compositional analysis via X-ray Fluorescence spectrometer and presented in Table 2. Table 2 presents the chemical composition of PLC, QP and sand via X-ray Fluorescence analysis. Chemical analysis revealed that QP and sand contained about 89.30 and 85.4 wt.% of SiO_2

respectively. The summation of alumina, silica and ferric oxide in QP was 91.10 wt.% hence the material satisfy to possess pozzolanic activity according to ASTM C 618 [45]. QP had a higher loss on ignition of 6.18 wt.% compared with sand' LOI of 0.27 wt.%. This could possibly be due to the presence of carbonates especially calcium carbonate evident from the chemical composition of QP. The high LOI of QP could be linked with the presence of carbonates. The lime content of 7.74 wt.% present in the QP composition met class F with CaO content < 10 wt.%. The sand' chemical composition indicated significant Fe_2O_3, Al_2O_3 and K_2O contents compared to QP, whereas the lime, sulphur contents and LOI were higher in QP compared with sand.

Table 3 indicates the effect of QP content and particle size on the water demand, initial and final setting times of cement blends whereas the effect of QP particle size and content on the water requirement at standard consistence for QP cement blends was illustrated in Figure 1.

An increase in the water consistence of the PLC blended with QP was observed as QP content was gradually replaced between 2.55 wt.% to 15 wt.% at various particle sizes. Similarly, particle size between 300 µm ~ 425 µm produced higher water consistence in comparison with other particle sizes. As the QP particle size was gradually decreased from the first fraction (1.19 mm ~ 2.0 mm) to the third fraction (300 µm ~ 425 µm) experienced increased water consistence whereas beyond sieve fraction of 300 µm ~ 425 µm resulted in a reduction in the water consistence at various cement replacements.

Table 2. Chemical composition of PLC, QP and Sand

Components	PLC wt.%	QP wt.%	Sand wt.%
SiO_2	12.39	89.30	85.42
Al_2O_3	4.20	1.72	9.15
Fe_2O_3	1.95	0.38	2.05
CaO	43.14	7.74	0.41
MgO	0.74	0.09	0.05
SO_3	1.03	0.50	0.08
K_2O	0.63	0.06	1.96
Na_2O	0.09	0.14	0.48
P_2O_5	0.18	0.01	-
Mn_2O_3	0.10	0.00	-
TiO_2	0.19	0.08	-
C_3S	50.42		
C_2S	–2.51		
C_3A	7.83		
C_4AF	5.93		
Silica Ratio	2.01	42.39	-
Alumina Ratio	2.16	4.49	-
Calcium Carbonate	79.00	16.75	-
L.O. I	34.67	6.18	0.27

Table 3. Effect of QP particle size and content on the setting times, normal consistence and water demand of PLC blends

QP Particle size	**Properties**	**2.5 wt.%**	**5 wt.%**	**7.5 wt.%**	**10 wt.%**	**12.5 wt.%**	**15 wt.%**
1.19 mm -2 mm	IST mins	96	103	108	122	130	143
	FST mins	210	221	233	245	257	268
	Consistency %	29	29	31	33	36	40
	Water demand mm	87	87	93	99	108	120
425 µm -1.19 mm	IST mins	106	112	118	133	147	165
	FST mins	232	245	256	268	281	301
	Consistency %	30.0	30.0	33.0	33.0	40.0	44.0
	Water demand mm	90	90	99	99	120	132
300 µm- 425 µm	IST mins	107	112	120	135	137	157
	FST mins	232	247	259	263	275	297
	Consistency %	32	33	36	41	45	46
	Water demand mm	96	99	108	123	135	138
212 µm- 300 µm	IST mins	118	128	140	148	161	160
	FST mins	236	241	250	263	273	268
	Consistency %	30.5	30	36	35	37	36.5
	Water demand mm	91.5	90	108	105	111	109.5
Below 212 µm	IST mins	121	130	144	153	167	169
	FST mins	239	245	253	261	277	279
	Consistency %	31	31.5	33	37	39	41
	Water demand mm	93	94.5	99	111	117	123

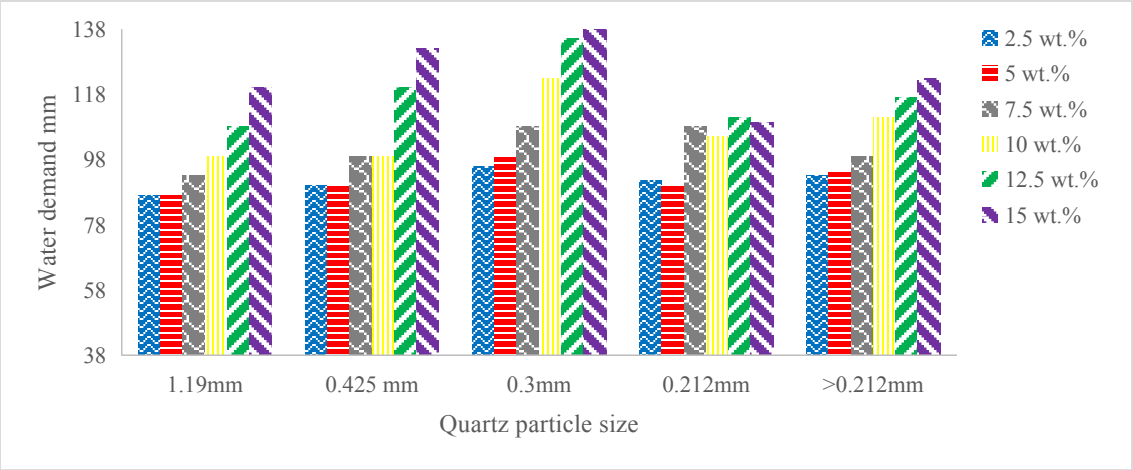

Figure 1. Effect of QP content on the water demand of PLC blend at various particle sizes.

Most of the QP-cement blend required more water demand for normal consistence especially beyond 5 wt.% of the various fractions. From Figure 1 it could also be seen that an increase in QP content resulted in an increase in the normal consistence for Q-PLC paste at various particle size. The water consistence of Q-PLC experienced an increase from 87 mm to 120 mm; 90 mm to 132 mm; 96 mm to 138 mm; 91.5 mm to 109.5 mm; 93 mm to 123 mm as QP content increased from 2.5 wt.% to 15 wt.%. Most of the cement blended with QP required more water for consistence compared to PLC as control. The QP possesses significantly high silica content with a low LOI of 6.18%. Excess of the silica could increase the water requirement for normal consistence according to Olubajo *et al.* [25].

This increased water requirement for normal consistence of the cement blended with QP compared with the control could be due to the high surface area of the QP [27,46] as well as the diminution of the clinker content by cement replacement according to Waziri and Olubajo [46]. Other reasons for increased water demand include excess silica content in the cement matrix [24] and formation of nucleation sites for CSH precipitation [47].

The initial and final setting time of PLC was 190 and 295 minutes respectively while the water consistence was 31% (93 mL). The inclusion of QP into the cement matrix resulted in an acceleration in the initial and final setting time values in comparison with PLC whereas as the cement was gradually replaced with QP from 2.5 wt.% ~ 15 wt.% resulted in a retardation at the various particle size. The quality of cement could be ascertained owing to the varying proportion of ingredients that comprises the cement blend. This decrease in the setting time (acceleration) in comparison with PLC as control could be attributed to the lower lime content requirement. The diminution of the clinker by replacement of cement with QP is responsible for the retardation in the setting time as the cement replacement was increased. The excess silica present in the cement blend leads to increase in the setting time (retarda-

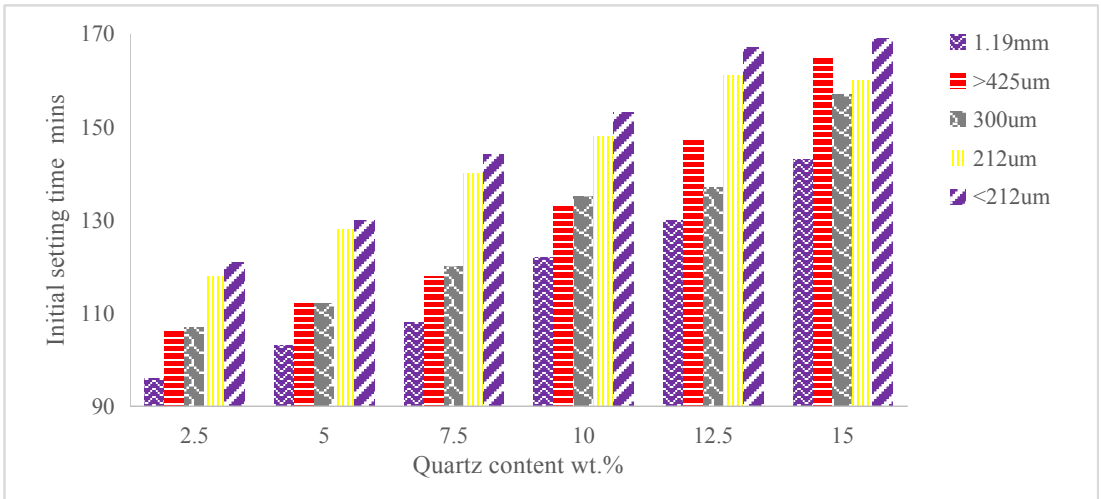

Figure 2. Effect of cement replacement on the initial setting time of PLC blends of various QP particle size

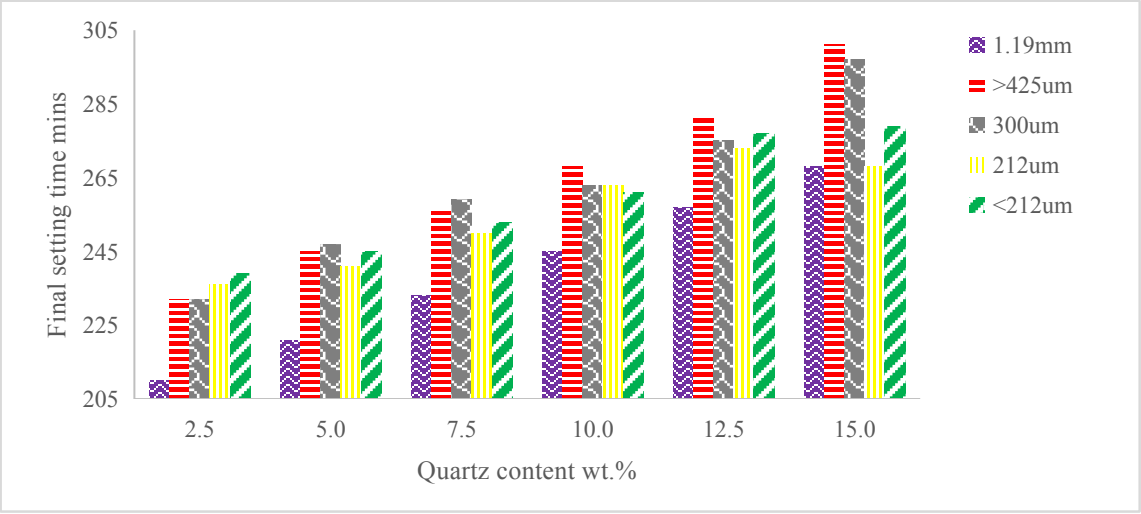

Figure 3. Effect of cement replacement on the Final setting time of PLC blends of various QP particle size

tion). Another reason for the elongated initial and final setting time could be linked with an increase in silica content which agrees with Zhu *et al*. [16] in which increase in the silica fume content led to a significantly elongation in its initial setting time results. Similar trend was observed for various particle sizes between: 1.19 mm ~ 2 mm, 425 µm ~ 1.19 mm, 300 µm ~ 425 µm, 212 µm ~ 300 µm and less than 212 µm respectively. It could also be observed that as the cement replacement level was increased from 2.5 wt.% ~ 15 wt.% at intervals of 2.5 wt.%, the initial setting time retarded from 96 ~ 143, 103 ~ 130, 108 ~ 144, 122 ~ 153, 130 ~ 167, 143 ~ 169 minutes respectively. It could be observed that as the cement replacement level with QP was gradually increased from 2.5 wt.% ~ 12.5 wt.% resulted in a gradual retardation in its setting time at various particle sizes.

Table 4 presents the effect of replacing PLC with QP at 0 wt.% ~ 15 wt.% at 2.5 wt.% interval. Results indicated that the specific gravity of cement blended with QP was lower than PLC employed as control. The decrease in the QP cement blends could be due to the lower specific gravity of the QP which agrees with Friedman *et al*. [8] resulting in lower specific gravity at higher cement replacement level. Since the specific gravity of the PLC is higher than QP.

Table 5 presents the effect of QP content on the mortar compressive strength of cement blends along with the mortar strengths of QP-cement blend expressed as a percentage rate of PLC at the same curing age. A reduction in the mortar compressive strength of PLC blended with QP was experienced as QP content was gradually increased between 2.5 wt.% ~ 15 wt.% at 2.5 wt.% interval. As the cement replacement level with QP content was increased from 0 ~ 15 wt.% resulted in a reduction in the 3-, 7-, 28- and 60-days strength by 85.1%, 67.5%, 63.9% and 70.8% respectively. This diminution in strength could be linked with the decrease in clinker content which is in agreement with Olubajo *et al*. [24] and Olubajo *et al*. [25] resulting in lower 28- and 60-days mortar compressive strength (63.9% and 70.8%) respectively.

Table 4. Variation of QP content on the Specific gravity of the various cement blends

QP wt.%	Specific gravity
0	3.07
2.5	3.05
5.0	3.04
7.5	3.03
10.0	3.02
12.5	3.01
15.0	3.00

Figure 3 indicates the effect of replacing PLC with QP on the mortar compressive strength as curing days progressed. From the compressive strength results, it could be deduced that most of the cement blends produced lower strengths in comparison with control except for 2.5 wt.% QP at curing age of 3 days which was 104.8% of the control strength at 3 days. This strength loss could be attributed to the diminution of the clinker content which is responsible for the formation of calcium silicate hydrate CSH, thus if the C_2S and C_3S content decreased resulting in lower strength which agrees with Waziri and Olubajo [46], Hossain *et al*. [48], Celik et al. [49], Kejela [50]. Similarly, as the curing age progressed from 3 to 60 days, the mortar compressive strength of cement blends as well as the control experienced increments of 53.36%, 32.52%, 50.82%, 20.43%, 43.02%, 43.68% and 27.63%. The increase in the

Table 5. Effect of QP content on the mortar compressive strength at various cement replacements

QP content wt.%	3 days (N/mm^2)	% Gain vs control gain	7 days (N/mm^2)	% Gain vs control gain	28 days (N/mm^2)	% Gain vs control gain	60 days (N/mm^2)	% Gain vs control gain
0	27.32	-	37.05	-	41.30	-	41.90	-
2.5	28.63	104.8	33.48	90.4	35.92	87.0	37.94	90.5
5	26.25	96.1	33.96	91.7	34.3	83.1	39.59	94.5
7.5	27.6	101.0	30.33	81.9	30.98	75.0	33.24	79.3
10	22.99	84.2	24.21	65.3	30.28	73.3	32.88	78.5
12.5	22.3	81.6	23.19	62.6	27.4	66.3	32.04	76.5
15	23.24	85.1	25.01	67.5	26.41	63.9	29.66	70.8

mortar compressive strength as curing age progress can be as a result of formation of more CSH as hydration of the cement matrix. Similar trends have been observed by Olubajo *et al*. [24], Olubajo *et al*. [25], Olubajo *et al*. [26], Waziri and Olubajo [46] and Olubajo *et al*. [51].

Another reason for lower strengths could be due to the high-water demand compared to control. At 28 days compressive strength for 2.5 wt.% and 5 wt.% QP, the cement blends attain 87% and 83.1% of the mortar compressive strength of the control. Thus, the optimal cement replacement with QP should not exceed 5 wt.%. considering early age of 3 days, the strength gain of between 2.5 wt.% (104.8%) and 7.5 wt.% (101.0%) produced significantly better strengths compared to control. Whereas beyond cement replacement of 7.5 wt.% resulted in significant strength loss.

At 2.5 wt.% QP-cement blend for curing ages of 3, 7, 28 and 60 days produced percentage compressive strength approximately 105%, 90%, 87% and 91% of the control' compressive strength respectively. The percentage mortar strength of 5 wt.% QP-cement blend in comparison with PLC at 3, 7, 28 and 60 curing ages were 96%, 92%, 83% and 95% respectively. For 7.5% QP-cement blend produced percentage compressive strength to control of 102%, 82%, 75% and 79% for 3, 7, 28 and 60 days respectively. For 10 wt.% QP-cement blend produced percentage compressive strength to control of 84%, 65%, 73% and 79% for 3, 7, 28 and 60 days respectively whereas for 12.5 wt.% QP-cement blend produced percentage compressive strength to control of 82%, 63%, 66% and 77%; for 15 wt.% QP-cement blend produced percentage compressive strength to control of 85%, 68%, 64% and 71% for 3, 7, 28 and 60 days respectively.

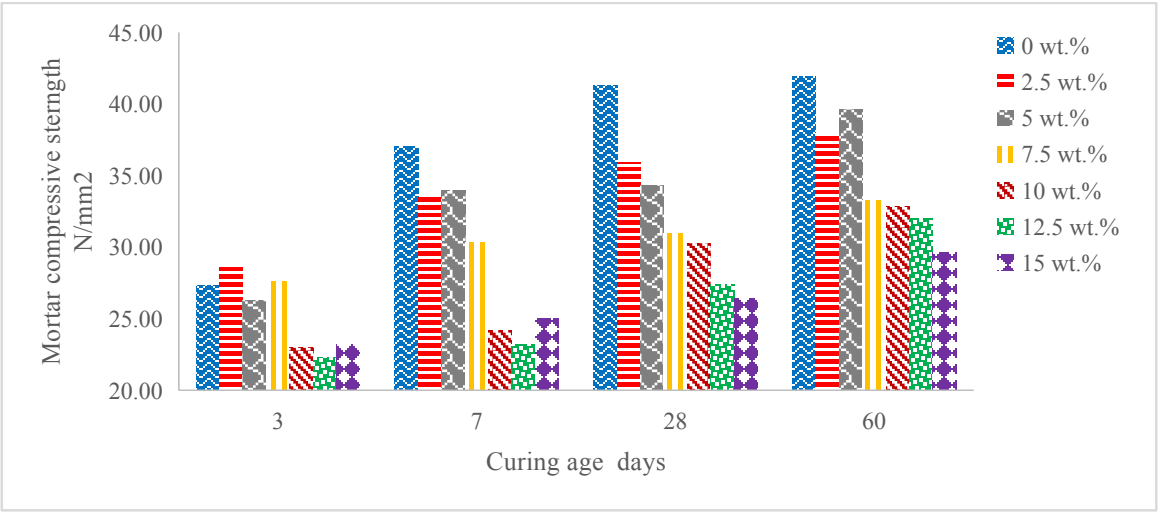

Figure 4. Effect of Curing age and QP content on the mortar compressive strength of cement blends

4. Conclusions

The following conclusions on the investigation of the effect of QP particle size and content on the cement properties are as follows: First of all, the QP chemical composition via X-ray fluorescence spectrometer indicated a significantly high silica content of 89.3 wt.%, alumina of 1.72 wt.% and Ferric oxide of 0.38 wt.% $SiO_2 + Al_2O_3 + Fe_2O_3$ (91.10 wt.%) which suggests that might possess pozzolanic properties according to with CaO content less than 10% at 7.74 wt.% which met Class F according to ASTM C618. Secondly, an increase in cement replacement with QP between 2.5 wt.% to 15 wt.% resulted in a reduction in its specific gravity. An increase in water consistence of QP-PLC blend occurred as cement was gradually replaced with QP at a given particle size. An increase in the QP surface area from 1.19 mm to 300 µm produced an increase in the water consistence of the cement blends ranging from 10.35 wt.% ~ 25 wt.% at a given cement replacement. Whereas for particle size below 300 µm produced higher water consistence in comparison with QP particle size of 1.19 mm. An increase in the water consistence of QP-PLC was experienced as the surface area of QP was enhanced at a given cement replacement. Thirdly, an elongation in the initial and final setting time was experienced as the particle size was enhanced (increased surface area), whereas an increase in cement replacement with QP content at given particle size resulted in a retardation in both setting times. This elongation in the setting time could be attributed to either clinker diminution or presence of silica. Finally, the mortar compressive strength of QP-cement blend experienced an increase as the curing age progressed at various cement replacements whereas, as the cement replacement level with QP content was gradually increased, resulted in a diminution in the strength in comparison with control. This could be linked with high water demand resulting in lower strengths coupled with diminution of the clinker content. The optimal QP content was determined at 5 wt.% owing to the fact that the physicomechnical properties did not significantly deviate from those of PLC as control. All the QP-cement blends fell within ASTM standards based on the cement properties.

Conflict of Interest

The authors declared that they have no conflict of interest.

Acknowledgments

The authors wish to thank Ashaka Cement Plc Nigeria and the departments of Chemical and Civil Engineering of Abubakar Tafawa Balewa University, Bauchi Nigeria for providing infrastructure, facilities and their support to this research work.

References

[1] Khan, M.N.N., Jamil, M., Karim, M.R., et al., 2017. Filler effect of pozzolanic materials on the strength and microstructure development of mortar. KSCE Journal of Civil Engineering. 21(1), 274-284.

[2] Soumya, G., Karthiga, S., 2018. Study on mechanical properties of concrete using silica fume and quartz sand as replacements. International Journal of Pure and Applied Mathematics. 119(14), 151-157.

[3] Zhang, H., Ji, T., Lin, X., 2019. Pullout behavior of steel fibers with different shapes from ultra-high-performance concrete (UHPC) prepared with granite powder under different curing conditions. Construction and Building Materials. 211, 688-702.

[4] Du, J., Meng, W., Khayat, K.H., et al., 2021. New development of ultra-high-performance concrete (UHPC). Composites Part B: Engineering. 224, 109220.

[5] Lin, R.S., Wang, X.Y., Zhang, G.Y., 2018. Effects of Quartz Powder on the Microstructure and Key Properties of Cement Paste. Sustainability. 10(3369), 1-16.

[6] Zuo, R.F., Du, G.X., Yang, W.G., et al., 2016. Mineralogical and chemical characteristics of a powder and purified quartz from Yunnan Province. Open Geosci. 8, 606-611.

[7] Afahnwie, N., Kedia, A., Suh, C., et al., 2022. The Potential of Quartzitic Veins in SW Cameroon for High-Purity Quartz. International Journal of Geosciences. 13, 281-302.

[8] Friedman, H., Koegel, D., Gilden, M., et al., 2014. Retrieved from http://www.minerals.net/GeneralInfromation.aspx.

[9] Obot, M.U., Yawas, D.S., Aku, S.Y., et al., 2016. An assessment on the production of abrasive sandpaper from locally sourced materials. Tribology in Industry. 38(2), 176.

[10] Collivignarelli, M.C., Ricciardi, G.C.P., Miino, M.C., et al., 2020. The production of sustainable concrete with the use of alternative aggregates: A review. Sustainability. 12, 7903.

[11] Dash, M.K., Patro, S.K., Rath, A.K., 2016. Sustainable use of industrial-waste as partial replacement of fine aggregate for preparation of concrete – A review. International Journal of Sustainable Built Environment. 5(2), 484-516.

[12] Li, C., Jiang, L., 2020. Utilization of limestone powder as an activator for early-age strength improve-

ment of slag concrete. Construction and Building Materials. 253, 119257.

[13] Moon, G.D., Oh, S., Jung, S.H., et al., 2017. Effects of the fineness of limestone powder and cement on the hydration and strength development of PLC concrete. Construction and Building Materials. 135, 129-136.

[14] Celik, K., Hay, R., Hargis, C.W., et al., 2019. Effect of volcanic ash pozzolan or limestone replacement on hydration of Portland cement. Construction and Building Materials. 197, 803-812.

[15] He, W., Liao, G., 2021. Effects of nano-CSH seed crystal on early-age hydration process of Portland cement. Fullerenes, Nanotubes and Carbon Nanostructures. 1-8.

[16] Zhu, J., Zhang, R., Zhang, Y., et al., 2019. The fractal characteristics of pore size distribution in cement-based materials and its effect on gas permeability. Scientific Reports. 9, 1-12.

[17] Lin, R.S., Wang, X.Y., 2021. Effects of cement types and addition of quartz and limestone on the normal and carbonation curing of cement paste. Construction and Building Materials. 305, 124799.

[18] Bezerra, A.C.S., Saraiva, S.L.C., Lara, L.F.S., et al., 2017. Effect of partial replacement with thermally processed sugar cane bagasse on the properties of mortars. Review of Materials. 22, 20. DOI: https://doi.org/10.1590/s1517-707620170 001.0117

[19] John, E., Matschei, T., Stephan, D., 2018. Nucleation seeding with calcium silicate hydrate–A review. Cement and Concrete Research. 113, 74-85.

[20] Bai, S., Guan, X., Li, G., 2022. Early-age hydration heat evolution and kinetics of Portland cement containing nano-silica at different temperatures. Construction and Building Materials. 334, 127363.

[21] Menezes, R.M.R.O., da Silva, R.M., Figueiredo, E.P., et al., 2018. Hydraulic binder obtained from recycled cement and sand powder. Revista IBRACON de Estruturas e Materiais. 11, 1178-1185.

[22] Yao, G., Cui, T., Zhang, J., et al., 2020. Effects of mechanical grinding on pozzolanic activity and hydration properties of quartz. Advanced Powder Technology. 31(11), 4500-4509.

[23] Kadri, E.H., Aggoun, S., De Schutter, G., et al., 2010. Combined effect of chemical nature and fineness of mineral powders on Portland cement hydration. Materials and Structures. 43, 665-673.

[24] Olubajo, O.O., Nuuman, A., Likita, N.S., 2020. The Effect of sugarcane bagasse ash on the properties of Portland limestone cement. American Journal of Construction and Building Materials. 4(2), 77-87.

[25] Olubajo, O.O., Isa, Y.M., Ayeni, S., et al., 2020. A Study on Ordinary Portland cement blended with Rice Husk Ash and Metakaolin. Path of Science. 6(1), 3001-3019. Available on website link: http://www.pos.org.

[26] Olubajo, O.O., Abubakar, J., Osha, O.A., 2020. The effect of eggshell ash and locust bean pod ash on the compressive strength of ternary cement. Path of Science. 6(3), 4001-4016. Available on website link: http://www.pos.org.

[27] Tavares, L.R.C., Junior, J.F.T., Costa, L.M., et al., 2020. Influence of quartz powder and silica fume on the performance of Portland cement. Scientific Reports.

[28] Tchamo, L.C.C., Libessart, L., Djelal, C., et al., 2020. Pozzolanic activity of kaolin containing aluminum hydroxide. Scientific Reports. 10, 2-13.

[29] Maljaee, H., Madadi, R., Paiva, H., et al., 2021. Incorporation of biochar in cementitious materials: A roadmap of biochar selection. Construction and Building Materials. 283, 122757.

[30] Saedi, A., Jamshidi-Zanjani, A., Darban, A.K., 2020. A review on different methods of activating tailings to improve their cementitious property as cemented paste and reusability. Journal of Environmental Management. 270, 110881.

[31] Olubajo, O.O., Osha, O.A., El-Natafty, U.A., et al., 2017. A study on Coal bottom ash and limestone effects on the hydration and physico-mechanical properties of ternary cement blends. Ph.D. Thesis. Abubakar Tafawa Balewa University, Bauchi, Nigeria. 1-305.

[32] Arroudj, K., Lanez, M., Oudjit, M.N., 2015. Characterization of cement mortar based on fine quartz, World Academy of Science Engineering and Technology. International Journal of Structural and Construction Engineering. 9(9), 1278-1281.

[33] Tikkanen, J., 2014. Effects of mineral powders on hydration process and hydration products in normal strength concrete. Construction and Building Materials. 72, 7-14.

[34] Popek, M., Sadowski, L., 2017. Selected physical properties of concrete modified using mineral powders. Procedia Engineering. 172, 891-896.

[35] Popek, M., Sadowski, L., 2017. Effect of selected mineral admixtures on mechanical properties of concrete. Key Engineering Materials. 728, 367-372.

[36] Popek, M., Sadowski, L., Szymanowski, J., 2016. Abrasion resistance of concrete containing selected mineral powders. Procedia Engineering. 153, 617-622.

[37] Ahmed, H.A.R., Mohamed, M., Mashaly, A.A., 2018. Mechanical and fracture mechanics properties of ultra-high-performance concrete. IOSR Journal of Mechanical and Civil Engineering (IOSR-JMCE). 15(5), 33-39.

[38] Galiska, A., Czarnecki, S., 2017. The effect of mineral powders derived from industrial wastes on selected mechanical properties of concrete. IOP Conference Series: Materials Science and Engineering. 245, 1-7.

[39] Borges, A.L., Soares, S.M., Taís Freitas, T.O.G., et al., 2021. Evaluation of the pozzolanic activity of glass powder in three maximum grain sizes. Materials Research. 24(4), 1-11.

[40] IS:4031(Part 4):1988-Methods of physical tests for hydraulic cement (Determination of normal consistence).

[41] IS:4031(Part 5):1988-Methods of physical tests for hydraulic cement (Determination of initial and final setting times).

[42] ASTM C 191, 2008. Standard test method for time of setting of hydraulic cement by vicat needle. Annual Book of ASTM Standards.

[43] ASTM C 187, 2010. Standard test method for normal consistency of hydraulic cement. Annual Book of ASTM Standards.

[44] ASTM C 109, 2008. Standard test method for compressive strength of hydraulic cement mortars. Annual Book of ASTM Standards.

[45] ASTM C 618, 2008. Standard specification for coal fly ash and raw or calcined natural pozzolan for use in concrete. Annual Book of ASTM Standards.

[46] Olubajo, O., Waziri, H., 2022. Potentials of Balanite Endocarp Pod ash as a cement replacement material. Journal of Building Material Science. 4(1), 44-53. DOI: https://doi.org/10.30564/jbms.v4i1.4800

[47] Kumar, A., Oey, T., Falzone, G., et al., 2017. The filler effect: The influence of filler content and type on the hydration rate of tricalcium silicate. Journal of the American Ceramic Society. 100(7), 3316-3328.

[48] Hossain, M.M., Karim, M.R., Hasan, M., et al., 2016. Durability of mortar and concrete made up of pozzolans as a partial replacement of cement: A review. Construction and Building Materials. 116, 128-140.

[49] Celik, K., Hay, R., Hargis, C.W., et al., 2019. Effect of volcanic ash pozzolan or limestone replacement on hydration of Portland cement. Construction and Building Materials. 197, 803-812.

[50] Kejela, B.M., 2020. Waste paper ash as partial replacement of cement in concrete. American Journal of Construction and Building Materials. 4(1), 8-13.

[51] Olubajo, O.O., 2020. The Effect of Eggshell Powder and Saw Dust Ash on the physico-mechanical properties of blended cement. American Journal of Construction and Building Materials. 4(2), 78-88.

[52] Suraneni, P., Weiss, J., 2017. Examining the pozzolanicity of supplementary cementitious materials using isothermal calorimetry and thermogravimetric analysis. Cement & Concrete Composites. 83, 273-278.

BILINGUAL PUBLISHING CO.
Pioneer of Global Academics Since 1984

Journal of Building Material Science
https://ojs.bilpublishing.com/index.php/jbms

ARTICLE

Impact of Polymer Coating on the Flexural Strength and Deflection Characteristics of Fiber-Reinforced Concrete Beams

Salih Kocak[1] **Kasim Korkmaz**[2*] **Erkan Boztas**[2]

1. University of West Florida, Pensacola, Florida, 32514, US
2. Construction Management Program, Eastern Michigan University, Ypsilanti, Michigan, 48197, US

ARTICLE INFO

Article history
Received: 6 December 2022
Revised: 23 December 2022
Accepted: 9 January 2023
Published Online: 12 January 2023

Keywords:
Concrete coating
Liquid polymers
Flexural strength
Deflection
Magnetic induction

ABSTRACT

Liquid polymers (LP) have become an important structural material used in the construction industry in the last decade. This paper investigates the viability of using commercially available LPs as a coating material to improve the flexural strength of fiber-modified concrete beams. The scope included preparing rectangular prism concrete beams with a concrete mixture including fly ash and fiber and coating them with four different liquid polymers at a uniform thickness following the curing process while one set of samples was maintained under the same conditions as a control group without coating. In addition, cylindrical samples were prepared to determine the compressive strength of the concrete mixture. Following the curing process in an unconfined open-air laboratory environment for another 28 days, concrete samples were tested to determine the flexural strength and deflection characteristics under center point loading equipment. The results revealed that all four coating types enhanced both the flexural strength and the average maximum deflection of the beams compared to the control group. While the enhancement in the flexural strength changed approximately between 5% and 36% depending on the coating type, the improvements in average maximum deflections varied between 3.7% and 28.4%.

1. Introduction

Concrete is used practically in any construction project, from buildings and roads to bridges and dams. With approximately 30 billion tons of annual consumption, it is the most used construction material all over the world [1,2]. For this purpose, it has been a major research topic for decades. Once designed, produced, and constructed properly, concrete is a very durable construction material and should not have any durability issues during its life cycle [3]. On the other hand, it was shown by experience that the desired long-term performance has generally not been accomplished due to the early failure of concrete structures [4]. As a naturally porous material regardless of the mix design, the durability of structural concrete is affected by mixture composition as well as the surface characteristics [5-7].

*Corresponding Author:
Kasim Korkmaz,
Construction Management Program, Eastern Michigan University, Ypsilanti, Michigan, 48197, US;
Email: kkorkmaz@emich.edu

DOI: https://doi.org/10.30564/jbms.v4i2.5304

Similar to concrete, polymers are being used almost in any phase of construction projects. It is mostly used to repair concrete work in the construction industry due to its durability, low permeability, high strength, and resistance to freeze and thaw characteristics. The use of polymers in concrete for various applications has been gaining popularity in the construction industry. There are three such applications commonly used nowadays, namely, polymer concrete, polymer-modified concrete, and impregnated concrete. In polymer concrete, cementitious materials inside ordinary concrete are completely replaced by polymers, commonly polyester styrene, acrylics, and epoxies., and cured at a certain temperature level [8]. Polymer-modified concrete, which is acquired by integrating very limited type polymers such as polymer dispersions, and water-soluble polymers, into the concrete during the mixing phase can benefit from the positive change in water/cement ratio and increased workability by lubrication effect [9]. They limit or eliminate the movement of water as well as the spread of the micro-cracks available in concrete [10]. In polymer-impregnated concrete, the liquid polymer fills the voids in concrete by replacing the free water and forms a solid polymer that fills following the heat-curing process [11]. Thermoplastic polymers are most used to impregnate concrete [9]. With this process, the compressive strength of the concrete was enhanced three to four times more than the conventional Portland cement concrete [9]. According to American Concrete Institute, the optimum polymer amount should be calculated and used in the polymer-modified concrete since the excess or deficit polymer amount can create adverse effects on the concrete itself by creating air entrainment or decreasing the water-reducing properties, respectively [10]. However, their use has been limited due to relatively higher costs and softening effects under high temperatures [9]. Polymer coating of concrete is similar to polymer impregnation of concrete. However, it is only performed on the visible surfaces of concrete structures. The use of surface coatings, which works as an impervious barrier between the surface of concrete and the surrounding environment, has been an effective way to safeguard existing and new structures made out of concrete [3,12,13]. However, there are no established criteria to assess the performance and selection of the appropriate coating material for exposure conditions [14]. There are various polymer-based surface coatings in the concrete industry such as acrylics, urethanes, and epoxy, to improve certain characteristics. As technology advances, the polymer manufacturing process enhances and facilitates the use of polymers in a wide range of construction projects. For example, some studies focused on glass and carbon fiber-reinforced polymer coatings to reinforce concrete and masonry structures against blast loads [15,16] while some other researchers investigated the hydrophobic [17], self-healing [18,19] and waterproofing [20] properties of the polymer coatings. Some other studies explored the effectiveness of fiber-reinforced polymer coatings in retrofitting damaged concrete beams [21]. Most recent studies related to concrete coatings focus on the durability of concrete, protection against corrosion, and chemically aggressive environments to achieve the expected service life. The impact of concrete surface coating on the mechanical properties, especially the strength and deformation characteristics has not been investigated thoroughly. This paper tried to fill the gap by evaluating the flexural strength and deflection characteristics of fiber-reinforced short concrete beams coated using commercially available liquid polymers.

2. Objectives and Scope

Concrete is the second most used material on the earth following water. It used more than twice the amount of all other construction materials combined mainly thanks to its strength and affordability. The strength of concrete is lessened over time due to aging-related deterioration under various climatic and loading conditions. The strength of concrete is typically determined by the type and proportioning of its fundamental ingredients, and practically it cannot be increased once the hardening process is completed. The purpose of this research is to examine the impact of liquid polymer (LP) coating on the flexural strength and deflection characteristics of fiber-reinforced concrete beams (FRCBs). The objective of this study includes evaluating the flexural strength values of FRCBs after coating with four different commercially available liquid polymers at the optimum coating thickness. The scope of the research covers preparing 6” by 12” cylindrical samples to determine the characteristic compressive strength of the mixture and 6” by 6” by 21” rectangular prism samples to evaluate the flexural strength of control and coated mixtures. Four different commercially available LPs are used in this research. In addition, four different flexural strength replicates are prepared per LP. Non-destructive magnetic induction method is utilized to measure the coating thickness to ensure a uniform polymer coating thickness on each sample. The deflection and the loading data are recorded throughout the testing until the samples failed.

3. Materials and Methods

3.1 Materials

Materials used in this study were mainly obtained from

local suppliers in the State of Michigan. The cement was selected as the commercially available type 1 Portland cement with a specific gravity of 3.15 g/cc and a specific surface area of 3,150 cm^2/g. The initial and final setting times were 1 hour 50 minutes and 3 hours 40 minutes, respectively.

The water used for hydrating the concrete mixtures and curing concrete samples was the potable water provided by the City of Ypsilanti with an average pH value of 7.07. Crushed coarse aggregates with at least two angular faces and a nominal maximum aggregate size (NMAS) of 19 mm were selected while the fine aggregates composed of natural and crushed sand were used in the concrete mixes. To match the job mix formula gradation, 6.5% lime filler was added to the fine aggregate portion. Combined gradation information of the aggregates along with some other physical properties of both aggregate types are provided in Table 1.

Table 1. Gradation and physical properties of aggregates.

Sieve Size (ASTM E11)		Percentage Passing
Standard	Alternate	
25.0 mm	1 in.	100
19 mm	3/4 in.	96.1
12.5 mm	1/2 in.	82.7
9.5 mm	3/8 in.	71.3
4.75 mm	No. 4	60.6
2.36 mm	No. 8	47.1
1.18 mm	No. 16	31.1
0.6 mm	No. 30	20.9
0.3 mm	No. 50	13.0
0.15 mm	No. 100	8.6
0.075 mm	No. 200	4.4
Los Angeles Abrasion		27%
Nominal Maximum Aggregate Size (mm)		19
Dry Rodded Unit Weight of Coarse Aggregate		1646 kg/m^3 or 100.1 $lb./ft^3$
Specific Gravity of Fine Aggregates		2.639
Specific Gravity of Coarse Aggregates		2.662

To make a concrete mixture similar to the one used in the region's construction projects, fibers and fly ash were added to the mixture at certain percentages based on the concrete volumetric design and manufacturers' recommendations. Non-magnetic synthetic fibers were put in the concrete mixture to increase the flexural toughness of the beams produced. The fibers had an average length of around 50 mm with an equivalent diameter of 0.77 mm and a specific gravity of 0.91. Figure 1 illustrates the synthetic fibers incorporated into the concrete mix. Class C fly ash with a specific gravity of 2.52 and an average particle size of 15 microns replaced some of the cement in the mixture.

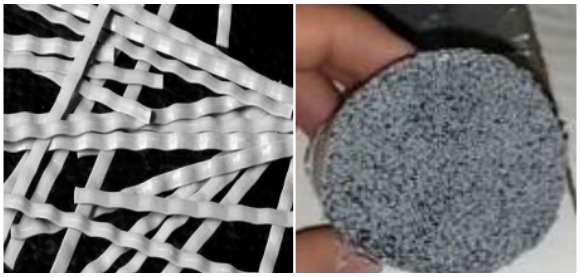

Figure 1. Synthetic fibers.

Liquid polymers used in this study were commercially available polyurethanes with the chemical name diphenylmethane di-isocyanates, water-based epoxy, and water-based organic polymer types. Since they are patented products, only certain information is available. Some of the chemical and physical properties provided by the manufacturer are given in Table 2.

Samples were maintained in a well-ventilated area following the application of the liquid polymer coatings to minimize the drying/curing time and avoid possible health hazards due to slight to mild odor.

3.2 Sample Preparation and Curing of Concrete Mixture

Single-source/single-batch materials, when possible,

Table 2. Properties of liquid polymers.

Analytical Properties	Value/ Characteristics			
	LP#1	LP#2	LP#3	LP#4
Color	Light Brown	Brownish	Extra White	White
Odor	Slight	Slight	Slight to Mild	Mild
Isocyanate Equivalent Weight	350	139	-	-
Viscosity @ 77 ^oF, centipoise	425	210	503	128
Specific Gravity @ 77 ^oF	1.16	1.23	1.42	0.99
Vapor Pressure @ 77 ^oF, (mm Hg)	$<10^{-5}$	$<10^{-5}$	$<10^{-5}$	$<10^{-5}$
Cleveland Open Cup Flash Point, ^oF	>230	>432	N/A	N/A
Solubility in water	Dilutable	Dilutable	Dilutable	Dilutable
Working time	Adjustable w/catalyst	4 hours	up to 8 hours	up to 24 hours

are used in the mix design to minimize the impact of source variability and focus merely on the impact of liquid polymers. Mix proportions are determined for a 4-inch slump following the absolute volume method. The water/cementitious material ratio was taken as 0.4, with cement occupying 9.3% of the mixture weight. Fresh concrete properties were measured to ensure consistency between the mixtures. The target air content was 6% and all samples had an air content changing between 5.2%-7.1%. The unit weight of the control concrete was 150.8 lb/ft^3 (pcf). Table 3 provides the concrete mix design proportions and per-sample weight in grams for the flexural strength samples.

Table 3. Concrete mix design proportions and per-sample weight.

Ingredients	Percentages in the mix	Per sample weight (gr)
Water (H_2O)	4.60%	1360
Cement (Type I)	9.30%	2720
Fly Ash (Class C)	2.30%	680
Fine Aggregates	27.90%	8160
Coarse Aggregates	55.70%	16330
Fiber (Synthetic)	0.15%	45
Total	100.00%	29295
water/cementitious	0.4	

Concrete ingredients were mixed in a laboratory-size concrete batching mixer to provide a uniform mixing for each sample. Ingredients were mixed for 5 minutes to obtain a homogeneous concrete mix. Lastly, the fibers were added to the mixer right after the mixing of the other ingredients was completed. As per the manufacturer's recommendation, the concrete was further mixed for another 70 revolutions to ensure the uniform distribution of the fibers throughout the concrete mixture. Following the mixing process, concrete was placed either into 6" by 12" cylindrical or 6" by 6" by 21" rectangular prism steel molds to prevent expansion. Cylindrical samples were placed into molds in three approximately equal layers whereas prismatic samples were placed in two equal lifts. Tamping and tapping of the layers for compaction, finishing and leveling the surface of the molds, and selection of the tools was performed according to the standard specification. Hardened concrete samples were unmolded and placed into a temperature-controlled circulatory water bath 24 hours after pouring the molds. Concrete samples were maintained in the water bath for another 28 days to complete the curing process as per standards. The temperature of the curing water was adjusted using a circulatory water heater at around 75^{o}F and when needed the water bath was topped with water to maintain the water level.

3.3 Application, Curing, and Thickness Measurement of Surface Coating

At the end of the curing period, some flexural strength samples were coated with liquid polymers whereas some prismatic samples were maintained as the control samples. The selection of samples to be coated and to be kept as control samples were performed randomly to prevent any sort of bias. Each polymer type was applied to 4 samples. Application of the liquid polymers was achieved using a roller brush. All four sides of the rectangular prism samples were coated with liquid polymers as shown in Figure 2.

Figure 2. Application of liquid polymer coating to rectangular prism concrete sample.

The number of roller passes per liquid polymer was investigated prior to the coating process to ensure the same thickness of the coating was applied to each sample. The thickness of the coatings was determined with an induction coating thickness gauge. Measurements were performed using the scan mode option, which allowed for checking the maximum, minimum, and average coating thicknesses on the entire surface. This process was repeated on four surfaces of all samples. The target coating thickness was set as 100 microns as per the literature. The coating thickness of all samples changed from 92 microns to 105 microns. While it took only 3 passes for the thickest liquid polymer to reach the target coating thickness, seven passes were applied to achieve the same coating thickness with a thinner liquid polymer. Hence, the number of passes ranged between 3 and 7 to reach approximately 100 microns of coating thickness. Following the coating, the samples were maintained in laboratory conditions for another 28 days before testing while the control samples were further cured during that time frame.

4. Performance Tests and Results

The flexural strength test was the main performance test conducted to determine the relative performance of the polymer-coated beams. The compressive strength of the unmodified concrete samples was also obtained for control purposes. Lastly, the change in deflection during the flexur-

al strength tests was recorded for all specimens to provide a comparison between various coatings of this study.

4.1 Compressive Strength

To acquire the characteristic compressive strength of the concrete mixtures, six cylindrical samples having a 6-inch diameter and 12-inch height were prepared. Tests were conducted using a test mark automated loading-controlled compression testing machine. Prior to the testing, the diameter and length of each sample were measured and recorded at least two different locations perpendicular to each other. Any sample with more than a 2% difference in diameter readings was discarded. In addition, if the end faces of the samples were not flat by more than 0.5 degrees, which was the case most of the time, they were ground to meet the standards. Once the samples were ready for testing, they were placed inside the unbonded caps and testing was performed by loading the samples 35±7 psi/s as per ASTM C39 standard specifications. The test continued until the sample was broken and the maximum load carried by the sample was captured automatically by the testing equipment. Subsequently, the compressive strength values of the samples were calculated by simply dividing the recorded maximum load in pounds by the average cross-sectional area calculated using the previously measured diameters. Since the length-to-diameter ratio of the samples tested was 2.0, there was no need to apply correction factors to the results. Table 4 provides compressive strength test data along with basic descriptive statistical analysis results. The design characteristic compressive strength was 4,500 psi. The average compressive strength obtained at the end of the tests was 4,972 psi with only a 0.6% coefficient of variation.

Table 4. Characteristic compressive strength.

Sample Number	Load at Failure	Compressive Strength
	lbf	psi
#1	140057	4953
#2	141630	5009
#3	139832	4946
#4	141181	4993
#5	139607	4938
#6	141181	4993
Average Compressive Strength		4972
Standard Deviation (psi)		30
Coefficient of Variation (%)		0.60%

4.2 Flexural Strength

The flexural strength of plain/unreinforced concrete is seen as an indirect measure of its tensile strength. It is more affordable and easier than a tensile strength test even though the results are slightly different. It can be defined as the ability of concrete to resist bending deformation under a flexure test. There are different flexural strength setups used to determine the modulus of rupture (MOR) of concrete beams. It is an important parameter for the design of concrete beam and slab-like structures. In this study, MoR values were determined under a mid-point (a.k.a center point or three-point) loading setup by testing 6" by 6" by 21" prismatic concrete samples. The test starts by laying the specimen centered horizontally over two points of contact on the bed of the testing machine. A single force applying contact point connected to the head of the testing machine just in the center point. Once the sample is ready to be loaded, a contact load in the range of 3% to 6% of the estimated maximum load is applied to the sample for the gap check between the specimen and any contact points. The specimen is loaded continuously without creating any shock. The loading is maintained at a constant rate throughout the test duration. The specification states that the loading should be applied in a way to create stress on the tension face at a rate between 125 psi to 175 psi. The following formula is used to calculate the rate of loading.

$$r = \frac{2*S*b*d^2}{3*L} \quad (1)$$

where,
r: rate of loading in lb/min
S: rate of increase in extreme fiber stress (psi/min)
b: average specimen width (inches)
d: average specimen depth (inches)
L: span length (inches)

The average depth and width of the specimen are determined after the testing is performed. There are three measurements taken for each dimension, one at the left end, one at the right end, and one at the center of the cross-section. 0.05 inches of precision is required in the dimension measurements as per the specifications. Once the testing is completed, Equation (2) is used to compute the modulus of rupture.

$$R = \frac{3*P*L}{2*b*d^2} \quad (2)$$

where,
R: modulus of rupture in psi
P: maximum applied load recorded by the testing machine in lbf
L: span length (inches)
b: average specimen width at fracture point (inches)
d: average specimen depth at fracture point (inches)

Table 5 summarizes the maximum loads both in pounds-force (lbf) and kiloNewton (kN) for each sample

that failed under the midpoint flexural strength test. Following the failure, samples were visually inspected for cracks, and width and depth measurements were taken from the cracked surface.

Similarly, Figure 3 illustrates the breaking loads in lbf as bar charts for (a) liquid polymer coating #1 (LP#1), (b) liquid polymer coating #2 (LP#2), (c) liquid polymer coating #3 (LP#3), and (d) liquid polymer #4 (LP#4), respectively. The red line in each graph corresponds to the average maximum load carried by control samples, which was equal to 5,593.25 lbf. All samples coated with liquid polymers carried higher loads compared to the uncoated samples other than LP#4- sample number (S#) 3, which carried only 54,66.4 lbf.

Table 5. Maximum load recorded during center point flexural strength test.

Specimen Type	Ultimate Load		Specimen Type	Ultimate Load	
	kN	lbf		kN	lbf
Control Sample#1	25.5	5721.4	Control Sample#2	24.3	5465.1
Coating LP#1-S#1	33.4	7515.4	Coating LP#3-S#1	28.6	6425.0
Coating LP#1-S#2	31.5	7077.0	Coating LP#3-S#2	28.6	6425.0
Coating LP#1-S#3	30.0	6739.8	Coating LP#3-S#3	31.5	7086.0
Coating LP#1-S#4	33.6	7546.8	Coating LP#3-S#4	28.9	6494.7
Coating LP#2-S#1	25.9	5811.3	Coating LP#4-S#1	29.9	6710.5
Coating LP#2-S#2	26.3	5912.5	Coating LP#4-S#2	27.9	6260.9
Coating LP#2-S#3	25.5	5721.4	Coating LP#4-S#3	24.3	5466.4
Coating LP#2-S#4	25.6	5750.6	Coating LP#4-S#4	26.4	5943.9

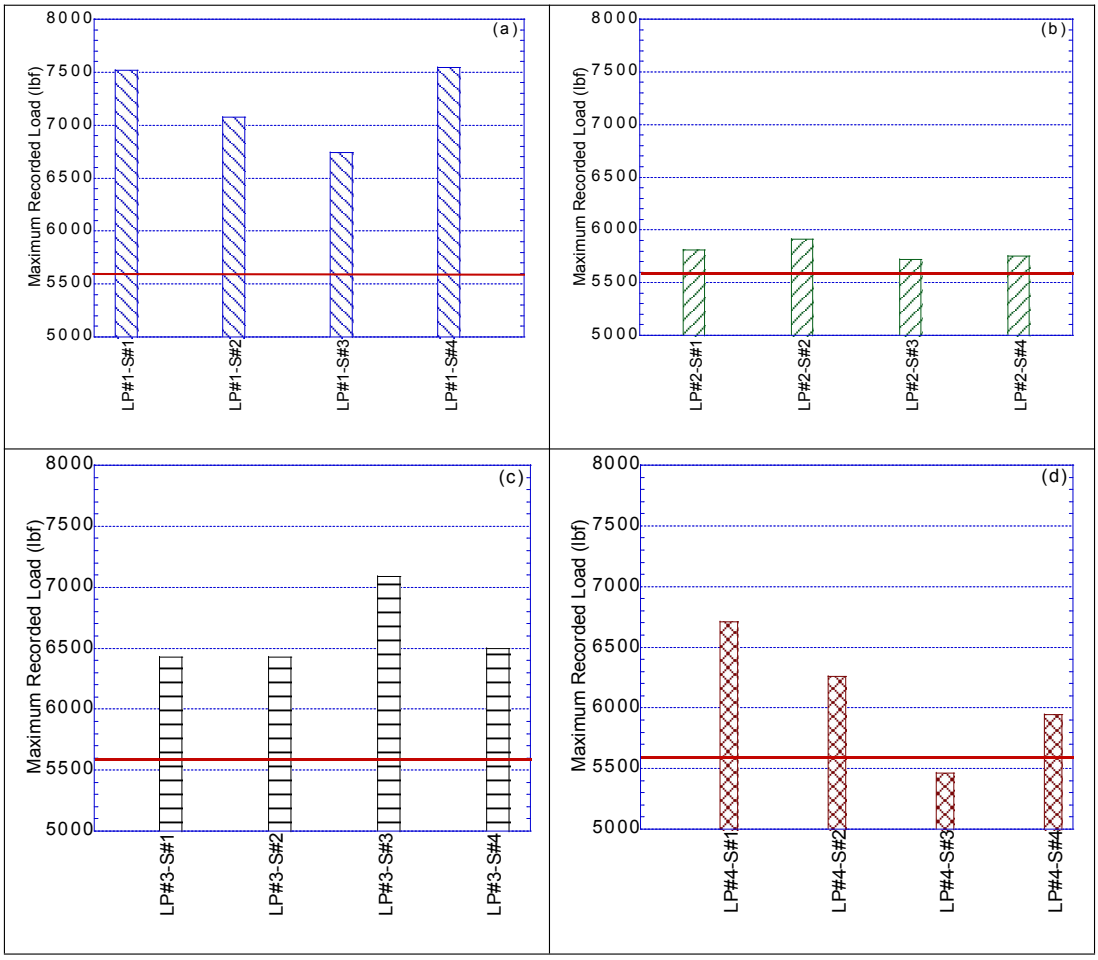

Figure 3. Maximum recorded load in psi for (a) liquid polymer#1 coating (b) liquid polymer#2 coating (c) liquid polymer#3 coating (d) liquid polymer#4 coating.

The flexural strength of the samples was calculated with the average width and depth of the prismatic samples obtained from broken cross sections using equation number 2. Following the modulus of rupture determination, the statistical significance test, also known as the t-test, was performed to determine the statistical significance of the test results. Tests were carried out between each group and results are provided in Table 6 along with an example t-test result table obtained between LP#1 and LP#2 mixture groups.

The P-value illustrated in bold in Table 6 is the most important result of the test. Since the t-tests were conducted based on a 95% confidence interval approach, the p-value less than 0.05 (5E-02) implies a statistically significant difference between the means of the trials. The bottom portion of Table 6 provided the p-values between each test group. According to the test result, there are statistical differences between the control and all coated mixtures as well as between all coated samples other than the LP#3 and LP#4 coatings, which yielded a p-value of 2.14E-1 > 5E-2.

Following the statistical significance test, basic statistical analysis was performed to determine possible outliers and/or extreme outliers. The rest of the data was used to conduct the descriptive statistical analysis for each coating type and control group. The average values per each data group along with the standard deviation bars are presented in Figure 4. The average, maximum and minimum values for the control group were marked in Figure 4 as well. Regardless of the liquid polymer coating type, all coatings improved the flexural strength values of the control mixture. In addition, the results illustrated that LP#1 coating improved the flexural strength of the concrete by around 264 psi, which corresponds to approximately a 36% increase compared to the control group. Similarly, LP#2, LP#3, and LP#4 advanced the modulus of rupture values by about 5%, 22%, and 17%, respectively.

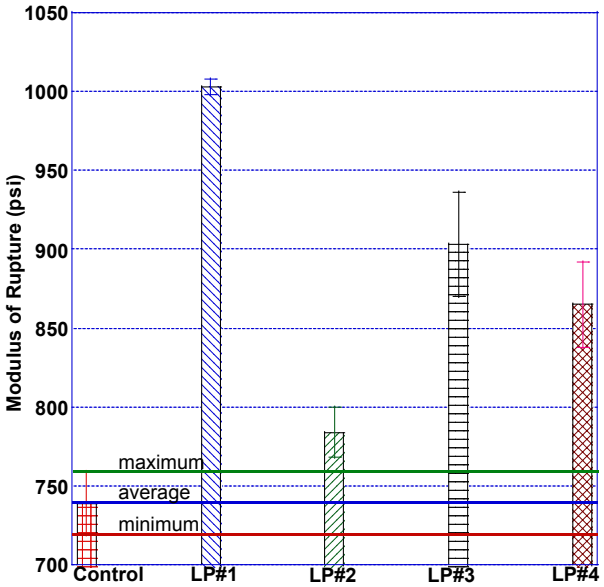

Figure 4. Average modulus of rupture (psi) values of control and liquid polymer coated prismatic concrete samples.

Table 6. t-test result between test groups with an example for LP#1 and LP#2.

t-Test: Two-Sample Assuming Equal Variances			**LP #1**	**LP #2**
Mean			967.9822287	773.5751073
Variance			1932.548475	268.4760421
Observations			4	4
Pooled Variance			1100.512259	
Hypothesized Mean Difference			0	
df			6	
t Stat			8.287618005	
P(T<=t) one-tail			8.35832E-05	
t Critical one-tail			1.943180281	
P(T<=t) two-tail			0.000167166	*Check <0.05*
t Critical two-tail			2.446911851	
LP#1 Coating	6.87E-05			
LP#2 Coating	2.63E-02	1.67E-04		
LP#3 Coating	1.90E-04	1.91E-02	8.00E-04	
LP#4 Coating	1.98E-03	1.24E-02	2.01E-02	2.14E-01

4.3 Deflection-Time

Serviceability is another important parameter that needs to be checked to ensure that concrete structures are stable. To meet the criteria set by the serviceability limit state, a concrete structure must remain serviceable throughout its design life by fulfilling its function. During the flexural strength test, other than the applied load, time and deflection values were also recorded. The change in deflection with time for each coating type is shown in Figure 5 along with the average deflection value obtained for the control mixture. Figures 5(a), (b), (c) and (d) illustrate the change in deflection with time for LP#1, LP#2, LP#3, and LP#4 samples, respectively. The deflection values were computed using the analytical approach to compare the recorded values. Equation (3) was applied to calculate the maximum deflection values.

$$\Delta max = \frac{P*L^3}{48*E*I} \quad (3)$$

where,

Δ_{max}: maximum deflection (in.)

P: maximum applied load recorded by the testing machine (lbf)

L: span length (in.), 18 in.

E: elastic/Young's modulus of concrete (psi), 4 million psi

I: Moment of inertia (in^4), approximately 108 in^4

The modulus of elasticity was calculated using the stress versus strain curves acquired during the compressive strength test. Based on the result, it was approximated to 4 million psi even though it showed minor changes

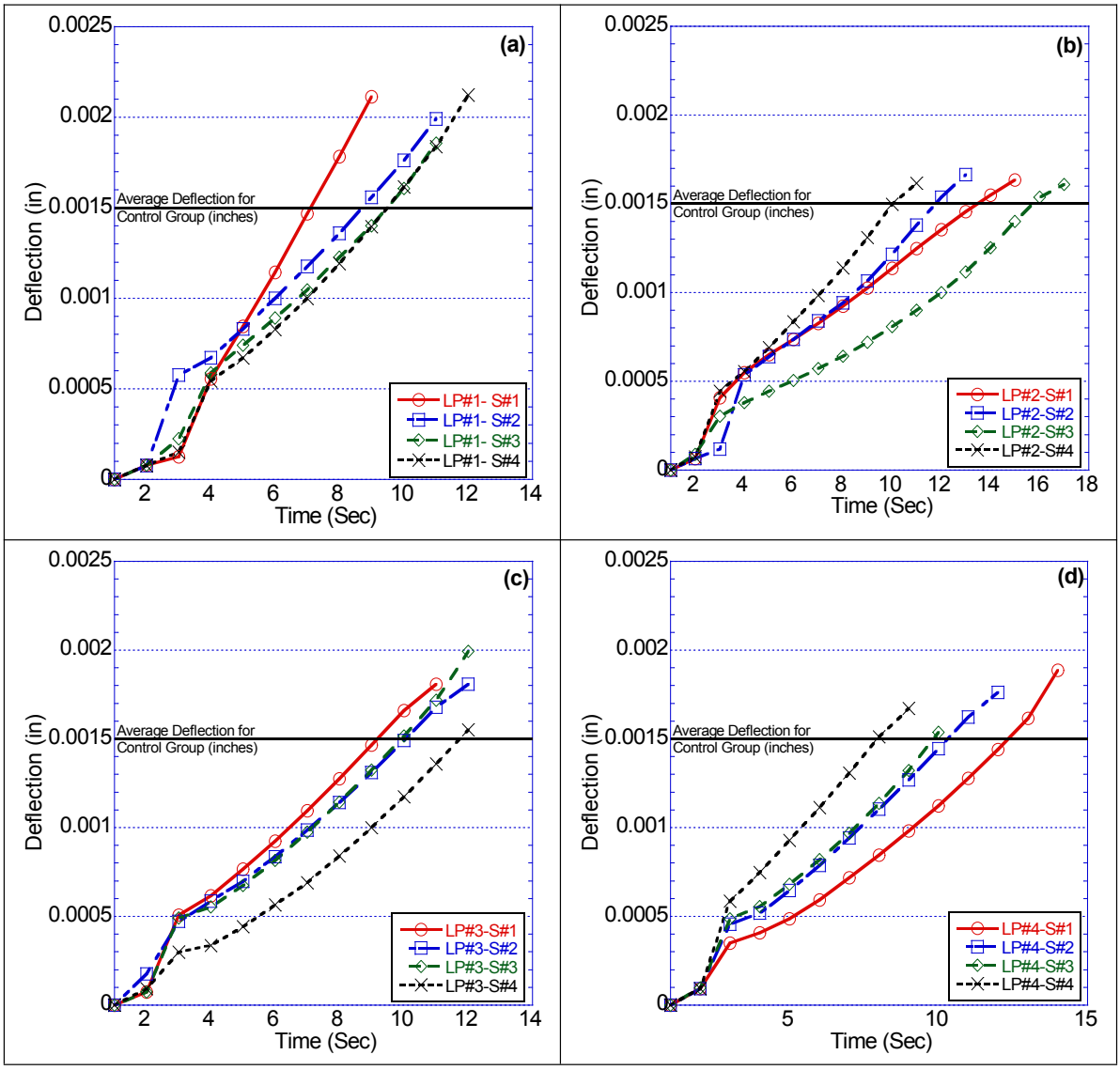

Figure 5. Change in deflection over time for (a) liquid polymer#1 coating (b) liquid polymer#2 coating (c) liquid polymer#3 coating (d) liquid polymer#4 coating.

per polymer coating type. Elastic modulus was taken to be the same for all samples tested. The moment of inertia, around 108 in^4, slightly changed for each sample depending on the average width and depth measurements. The span length was taken as 18 inches based on the distance between the support points of the testing apparatus.

Similar to the flexural strength test results, statistical significance tests, determination of outliers and/or extreme outliers as well as the descriptive statistical analysis were performed for deflection values. Table 7 summarizes both maximum and average deflection values for each coating type and control mixture group along with the percent change in deflection compared to the control mixture. The results show that polymer coatings improved the average deflection regardless of the coating type. While LP#1 coating increased the average deflection by 28.4% and maximum deflection by 27.0%, LP#2. LP#3 and LP#4 coatings enhanced the average deflection by 3.7%, 15.3%, and 16.0%, respectively.

Table 7. Maximum and average deflection values.

	Deflection (in)		**Change in Deflection (%)**	
	Average	Maximum	Average	Maximum
Control Group	0.001573	0.001672	-	-
LP#1 Coating	0.002021	0.002123	28.4%	27.0%
LP#2 Coating	0.001631	0.001664	3.7%	–0.5%
LP#3 Coating	0.001814	0.001827	15.3%	9.3%
LP#4 Coating	0.001824	0.001887	16.0%	12.9%

5. Conclusions & Recommendations

This research paper presented the findings of liquid polymer coating of fiber-reinforced concrete beams. Four commercially available polymer coatings with different physical properties were selected for this study. The flexural strength and deflection versus time characteristics using a mid-point test setup were determined to compare the impact of coatings relative to the control concrete mix design. Statistical significance tests were conducted to check if the results obtained were statistically different. The following conclusions can be withdrawn based on the results of this research study.

- The characteristic compressive strength with 4500 psi was designed and the average 28-day compressive strength of the mix design was obtained as 4972 psi.
- All liquid polymer-coated samples other than LP#4-S#3 carried higher loads than the uncoated/control samples.
- The statistical significance test results showed that all coated mixtures were statistically different from the control mixture based on a 95% confidence interval. Moreover, all coated mixtures other than between LP#3 and LP#4 were statistically different as well.
- Regardless of the coating type, all coatings enhanced the flexural strength values compared to the control mixture. While LP#1 coating achieved an average flexural strength increase of around 36%, LP#2, LP#3 and LP#4 coatings enhanced it by approximately 5%, 22%, and 17%, respectively.
- Similarly, all coating types improved the average deflection values. LP#1 coating increased the average deflection by 28.4% whereas LP#2. LP#3 and LP#4 coatings enhanced the average deflection by 3.7%, 15.3%, and 16.0%, respectively.

Conflict of Interest

There is no conflict of interest.

References

[1] Anonymous, 2021. Concrete needs to lose its colossal carbon footprint. The International Journal of Science. 597, 593-594.

[2] EMC Cement, 2022. The Scale of Concrete [Internet] [Accessed 2022 Nov 24]. Available from: https://lowcarboncement.com/the-scale-of-concrete.

[3] Aguiar, J.B., Camoes, A., Moreira, P.M., 2008. Coatings for concrete protection against aggressive environments. Journal of Advanced Concrete Technology. 6(1), 243-250.

[4] Rodrigues, M.P., Costa, M.R.N., Mendes, A.M., et al., 2000. Effectiveness of surface coatings to protect reinforced concrete in marine environments. Materials and Structures. 33, 618-626.

[5] Kropp, J., Hilsdorf, H. (editors), 1995. Performance criteria for concrete durability : State of the art report prepared by RILEM Technical Committee TC 116-PCD. Performance of Concrete as a Criterion of its Durability. E & FN Spon: London.

[6] Zhao, Z., Qu, X., Li, J., 2020. Application of polymer modified cementitious coatings (PCCs) for impermeability enhancement of concrete. Construction and Building Materials. 249, 118769.

[7] Ahmed, A., Guo, S., Zhang. Z., et al., 2020. A review on durability of fiber reinforced polymer (FRP) bars reinforced seawater sea sand concrete. Construction and Building Materials. 256, 119484.

[8] Li, Z., 2011. Advanced concrete technology. John Willey and Sons, Hoboken, NJ: USA.

[9] Deshrousses, R., Soliman, A. (editors), 2018. The

uses of polymers in concrete: Potentials and difficulties. Building Tomorrow's Society; 2018 Jun 13-16; Fredericton, Canada. Canada: CSCE SCGC.

[10] ACI committee 548, polymers in concrete, 2009. Report on Polymer Modified Concrete. American Concrete Committee Reports. ACI 548.3R-09. 1-40.

[11] Gambhir, M.L., 2008. Concrete technology. McGraw Hill Education: Patiala, India.

[12] Elsayed, M., Elsokkary, T., Shohide, M., et al., 2019. Surface protection of concrete by new protective coating. Construction and Building Materials. 220, 245-252.

[13] Chi, J., Zhang, G., Xie, Q., et al., 2020. High performance epoxy coating with cross-linkable solvent via Diels-Alder reaction for anti-corrosion of concrete. Progress in Organic Coatings. 139, 105473.

[14] Almusallam, A., Khan, F.M., Maslehuddin, M., 2002. Performance of concrete coatings under varying exposure conditions. Materials and Structures. 35, 487-494.

[15] Urgessa, G.S., Esfandiari, M., 2018. Review of polymer coatings used for blast strengthening of reinforced concrete and masonry structures. Taha, M. (editor) International Congress on Polymers in Concrete (ICPIC 2018). Springer: Berlin/Heidelberg, Germany.
DOI: https://doi.org/10.1007/978-3-319-78175-4_91

[16] Irshidat, M., Al-Ostaz, A., Cheng, H.D., et al., 2011. Nanoparticle reinforced polymer for blast protection of unreinforced masonry wall: Laboratory blast load simulation and design models. Journal of Structural Engineering. 137(10), 1193-1204.

[17] Liu, L., Zhao, P., Liang, C., et al., 2022. Assessment and mechanism of inorganic hydrophobic flake incorporated into a polymer-modified cement-based coating. Journal of Building Engineering. 60, 105185.

[18] Tran, N., Nguyen, T., Ngo, T., 2022. The role of organic polymer modifiers in cementitious systems towards durable and resilient infrastructures: A systematic review. Construction and Building Materials. 360, 129562.

[19] Cho, S., White, S.R., Braun, P.U., 2009. Self-healing polymer coatings. Advanced Materials. 21(6), 645-649.
DOI: https://doi.org/10.1002/adma.200802008

[20] Cho, B.H., Nam, B.H., Seo, S., et al., 2019. Waterproofing performance of waterstop with adhesive bonding used at joints of underground concrete structures. Construction and Building Materials. 221, 491-500.

BILINGUAL PUBLISHING CO.
Pioneer of Global Academics Since 1984

Journal of Building Material Science
https://ojs.bilpublishing.com/index.php/jbms

ARTICLE

Thermal Analysis of Concrete Mixtures with Recycled EPS Aggregates

Aisha Ayoubi[1] Emilio Sassine[1*] Joseph Dgheim[1] Joelle Al Fakhoury[1,2] Yassine Cherif[2] Emmanuel Antczak[2]

1. Lebanese University, Habitat and Energy Unit, Group of Mechanical, Thermal and Renewable Energies—Laboratory of Applied Physics (LPA-GMTER), Faculty of Sciences, Fanar Campus, Lebanon, 248199, France
2. Univ. Artois, IMT Lille Douai, Junia, Univ. Lille, ULR 4515, Laboratoire de Génie Civil et géo-Environnement (LGCgE), F-62400 Béthune, France

ARTICLE INFO

Article history
Received: 15 November 2022
Revised: 28 November 2022
Accepted: 20 December 2022
Published Online: 7 February 2023

Keywords:
Concrete mixtures
Hollow blocks EPS beads
Thermal properties
Thermal insulation
Recycled wastes

ABSTRACT

Reusing recycled waste materials in buildings is gaining more and more attention for what it offers economic, environmental, and energy benefits; and many researchers are nowadays working on producing new sustainable construction materials incorporating recycled wastes. In this scope, this work uses an experimental approach aiming at understanding the effect of incorporating Expanded Polystyrene (EPS) beads in concrete and proposing thermally improved concrete mixtures for the production of hollow blocks in Lebanese constructions by substituting fine aggregates with recycled products such as EPS in order to promote their insulating properties. Three different diameters of EPS beads (2 mm ~ 3 mm, 3 mm ~ 4 mm and 4 mm ~ 5 mm) are studied with different volumetric ratios (20%, 40%, 60% and 80%) in order to investigate the effect of EPS on the thermal properties of concrete. The results showed that the only the percentage of incorporated EPS beads impacted the thermal performance of the concrete mixtures while the EPS diameters have a negligible effect on the thermal properties of the concrete samples.

1. Introduction

Buildings are globally accountable for a paramount depletion of energy. Inside them, electrical power is used for an extensive variety of applications. One of the applications is a direct relation to the equipment required to deliver thermal comfort to occupants, which may be responsible for a significant amount of whole-building energy consumption. The amount of power needed by HVAC (Heating, Ventilation and Air Conditioning) systems rely on many factors and, one of the major factors is the conduction load via the building envelope. A report by the International Energy Agency [1] suggests that the current energy usage on heating and/or cooling on account

*Corresponding Author:
Emilio Sassine,
Lebanese University, Habitat and Energy Unit, Group of Mechanical, Thermal and Renewable Energies - Laboratory of Applied Physics (LPA-GMTER), Faculty of Sciences, Fanar Campus, Lebanon;
Email: emilio.sassine@ul.edu.lb

DOI: https://doi.org/10.30564/jbms.v4i2.5251

of thermal comfort consists of 60% of global energy consumption in buildings. With the need for energy that is assumed to be tripled by 2050, it is essential to concentrate on initiating techniques to either create clean, eco-friendly energy or limit the energy needs in buildings. One of the appropriate ways for the latter approach is to generate contemporary construction materials with magnified insulating properties to reduce the heat flow in and out of the buildings, consequently cutting down the necessity for energy needed to preserve indoor thermal comfort.

Concrete masonry blocks are largely used in building envelopes for what they offer as advantages such as their low cost, their low maintenance, their ease of implementation, and their fire resistance [2]. However, one of the biggest drawbacks of this technology is its relatively low thermal performance, which makes concrete blocks need lots of improvements to meet the recent requirements in terms of energy efficiency and comfort.

Hollow concrete blocks can be thermally enhanced by either adding insulation materials into their cavities, by modifying their shapes (modifying the shapes of the cavities, adding bulkheads, increasing the thickness of the block), or by incorporating some materials into the concrete mixture composition.

In the last couple of years, deep research attempts have been done in order to recycle wastes for probable utilization for the manufacturing of concrete services [3]. That's the reason why the blocks of concrete have been considered the best choice for the consolidation of recycling materials from waste due to its small amount of quality needs materials. One of the major components in the concrete block is known as Aggregate, which contributes to 80% of the complete volume. It is very crucial in affecting the blocks of concrete characteristics. As long as the traditional aggregate utilization does not serve the environment and will lead to a reduction of normal assets as it is stated by Medina et al. [4]. The wide range of materials generated from waste has been reproduced in which it will be utilized as aggregate in the concrete block's manufacturing.

Yoshida et al. [5] have stated that the universal disposal of cathode ray tubes (CRT) is able to gain its maximum in the following five years between 2015 and 2020. And that will make the government put a massive effort to discover a reasonable option for CRT waste disposal. As has been investigated by Zhang et al. [6], a massive quantity of waste from plastic materials has been released and neglected in landfills. They have also stated that these wastes should be used in construction services.

Medina et al. [4] have studied the use of ceramic waste as aggregate during the manufacturing of concrete blocks. They have discovered that it has many beneficial characteristics such as long service life, massive resistance from abrasion resistance as well as fire and heat resistance. Furthermore, the elevated insulation characteristics such as thermal insulation are considered the most significant benefit of the use of Crumb Rubber (CR) during the manufacturing of concrete blocks. Mohammed et al. [7] have also stated that conventional block of concrete has greater thermal conductivity compared to CR concrete blocks. In fact, expanded polystyrene (EPS) which is classified as an ultra-lightweight aggregate is one of the promising aggregates, owing to its properties of ultra-low density, thermal insulation and energy absorption compared to ordinary concrete. According to Chen et al. [8], restricted crushed waste from EPS straight in concrete has been used as it is known as the most economical usage of EPS.

Khatib et al. [9], and Bhutta et al. [10], declared that EPS has been utilized as an insulating material, due to its low density, thermal insulation, nonabsorbent as well as its low cost. During the experimental work of Khatib et al. [11], the thermal properties of the natural aggregates were achieved using EPS in order to reduce costs and protect the environment. Emilio et al. [12] studied the influence of adding EPS beads to the concrete mixture. Four different hollow block samples were produced using different EPS ratios (0 g, 6 g, 12 g, and 18 g) and tested in order to find their thermal resistances. As a result, they found that the outcome was encouraging in terms of a thermal point of view, where adding 18 g of EPS beads increased the thermal resistance from 0.16 m^2KW^{-1} to 0.31 m^2KW^{-1}.

Ganesh et al. [13] used two different sorts of EPS beads in their investigation with various dimensions of 4.75 mm ~ 8 mm having a bulk density of 9.5 kg/m^3, and 2.36 mm ~ 4.75 mm with a bulk density of 20 kg/m^3. Their study indicates that the EPS concrete mixes manufactured with processed fly ash represent less water absorption amounts in comparison with the usual concrete material. Sayadi et al. [14] have focused on the influence of EPS particles on the fire resistance of foamed concrete as well as the thermal conductivity, and they discovered that when the volume of EPS increases, the fire resistance, as well as the thermal conductivity of the concrete decreases.

Moreover, the concern for the environment which has been related to the disposal of different types of waste materials has increased at an alarming rate. Annually, various kinds of waste have been produced in massive amounts depending on local industries. Consequently, the need for further sustainable procurement has increased the necessity of constructing a green environment.

As it is mentioned in the research of Karade [15] and Xuan et al. [16], massive quantities of waste materials generated are either burnt or landfilled and this leads to con-

tamination as well as environmental pollution. As a result, there is a huge pressure applied to enhance the reuse value of waste materials. Besides this, it is found that the use of crumb rubber leads to better insulation properties and improved toughness, while the insertion of waste glass aggregate improves the values of concrete blocks [17,18].

The aim of this work is to investigate the thermal advantages of producing concrete mixtures with EPS beads aggregates as a substitution for stone aggregates.

For this purpose, different cubic samples (10 cm × 10 cm × 10 cm) were produced with different beads diameters and different EPS volumetric rations in order to assess and compare the influence of these two parameters on the thermal performance of the concrete mixtures using experimental measurements.

The thermal study is complemented and supported by an economic and environmental evaluation of the analyzed samples in order to stress the feasibility and sustainability of the proposed technology.

2. Experimental Approach

2.1 Preparation of the Concrete Mixtures

2.1.1 EPS Beads Properties

The polystyrene beads were provided by a local Lebanese supplier with three different nominal diameters (3 mm, 4 mm, and 5 mm). In order to have a better accuracy, the EPS beads diameters and masses were first determined in order to calculate their density on the one hand, and also to determine the mass required to reach the required volumetric ration on the other hand.

A caliper was used for measuring the average diameter of the polystyrene aggregates and ten measurements were performed from each EPS beads bag (Figure 1); also, the ten beads from each category were weighed using a digital balance (Figure 2).

The average values of the ten measurements for the different nominal diameters are reported in Table 1.

Figure 1. Three different dimensions of EPS aggregates.

The volume and density of EPS beads aggregates are calculated using the following equations:

$$V = \frac{4}{3}\pi r^3 \quad (1)$$

$$\rho = \frac{m}{V} \quad (2)$$

Figure 2. Mass determination using a digital balance.

Table 1. Properties of EPS beads.

EPS dimension (mm)	3	4	5
Average diameter (mm)	2.668	3.955	4.897
Average mass (g)	0.00032	0.0009	0.00155
Average volume (mm^3)	9.94	32.37	61.45
Average Density (g/L)	32.2	27,78	25.22

2.1.2 Preparation of the EPS Concrete Samples

The mixtures were studied according to two parameters, the amount of EPS beads aggregate (percentage of lightweight aggregate volume with respect to the total concrete volume) and the diameter of EPS beads. Four different volumetric ratios were used (20%, 40%, 60% and 80%), and three different diameter categories (3 mm, 4 mm, and 5 mm); this results in twelve different EPS concrete mixtures (C2-C13) with one reference concrete mixture without EPS aggregates (C1).

The ingredients used to prepare the concrete reference mixture (C1) are: 350 g of type 1 cement, aggregates used in two sorts (700 g of sand and 1050 g of crushed dust) and the amount of water used during the mix 300 g. These ingredients are generally used to prepare the concrete mixtures of traditional Lebanese hollow blocks and were used in this experiment to prepare the reference sample cube (C1). This concrete mixture has a density of 1400 kg/m^3 and a water-cement ratio ratio r/c is 0.6.

In the twelve remaining concrete EPS mixtures (C2-C13), EPS beads were used as a substitution to stone aggregates in different diameters (2 mm ~ 3 mm), (3 mm ~ 4 mm) and (4 mm ~ 5 mm) and in different volumetric proportions of 20%, 40%, 60% and 80%. The amount of cement used for all cubes is the same whereas the amount for aggregates differs from one cube to another depending on the number of EPS added (Table 2).

Figure 3a shows the materials used to prepare our mix design, whereas Figure 3b displays how the sand is sieved over 4.75 mm in order to be used during the mix preparation. The ingredients were very well mixed to guarantee as

Table 2. Cubes characteristics.

	EPS Diameter (mm)	Volumetric EPS percentage (%)	Cement (g)	Water (g)	Crushed dust (g)	Sand (g)
C1	-	-	350	300	1050	700
C2	2-3	20	350	300	945	630
C3	2-3	40	350	290	840	560
C4	2-3	60	350	280	735	490
C5	2-3	80	350	270	630	420
C6	3-4	20	350	300	945	630
C7	3-4	40	350	290	840	560
C8	3-4	60	350	280	735	490
C9	3-4	80	350	270	630	420
C10	4-5	20	350	300	945	630
C11	4-5	40	350	290	840	560
C12	4-5	60	350	280	735	490
C13	4-5	80	350	270	630	420

(a) (b) (c)

Figure 3. Materials preparation (a), aggregate (Sand) sieving (b), and mix preparation (c).

much as possible the homogeneity of the mixture (Figure 3c). The following step is to weigh all the required materials using a digital balance. Then, we use a steel bowl to mix all the materials.

Figure 4a shows how the materials are mixed using a concrete mixer. All the materials are mixed approximately for two minutes. Then they are stopped and rested for roughly one minute. The following step is to use a small spoon to mix all the materials properly and gently. Afterward, we turn on the mixer to mix the materials for another two minutes. Then, we remove the steel bowl from the concrete mixer in order to check if the materials are ready for the next step which is preparing all required concrete cubes as it is shown in Figure 4b.

(a) (b)

Figure 4. Concrete mixer (a) and concrete mixture (b).

After preparing the concrete mix, the cubic samples were made by pouring the concrete mixtures into the cubic formworks. After proper lubrication of the formwork to avoid any cracking when demolding, the cubic formwork was filled in three layers with 25 blows per layer. The third layer was finished with a nice and flat upper surface.

After finishing the pouring phase, the cubes were covered with a plastic bag and a rubber band to make them tight enough and stored in a room temperature environment. After 24 hours, the cubes were watered by adding half a cup of water to each sample once every day for approximately four days to avoid any cracking. Then the samples were tested after 14 days after the preparation of the mixtures to make sure they reached their final thermophysical properties. Figure 5 shows the first cube with no EPS added and the other 12 cubes which are made using different percentages as well as different diameters of EPS.

2.2 Thermal Characterization of the Concrete Mixtures

2.2.1 Thermal Experimental Setup

In order to investigate the thermal performance of the prepared samples using the flux metric method (NF EN 12939) [19] for the characterization of the thermal performance, an in-house manufactured thermal characterization setup is used. A water tank is left at ambient temperature while the other one is heated to 50 °C. The hot water is circulated to the bottom heat plate through a circulating pump and the tested samples are sandwiched between the two heat plates; a thermocouple and flux meter are placed straight under the sample and another thermocouple is placed over the sample (Figure 6). The fluxmeter and the two thermocouples are connected to a data acquisition of an electronic system to record the evolution of the heat flux φ and the temperatures T_1 and T_2. Each water tank is left for about one hour to warm up before recording any experimental data. Then, all data are recorded and each test is done three times in order to clarify the stability and the accuracy of the results. The heat flux increases gradually, then it decreases slightly until it becomes stable. Each test takes approximately 120 minutes before stability occurs. All the experimental components are placed in an insulated chamber and the tested samples are wrapped laterally with mineral wool insulation material in order to decrease the lateral heat losses and insure unidirectional heat transfer. The type of heat flux which is used during the experiment is known as HPF01 as it is used to estimate the heat flux through the object in $W \cdot m^{-2}$. As for heat flux measurement in buildings and soil, HFP01 is known as the most popular sensor. This sensor is very stable and strong. In order to determine the difference in temperature, the sensor in HPF01 which is known as thermopile is used. The thermopile is known as a passive sensor that does not need any power. However, in order to find out the heat flux, the output of HPF01 (small voltage) is divided by the sensitivity which has been equal to 62.51 $\mu V \cdot W^{-}1 \cdot m^{-}2$. In addition, the temperature interval is ranged between –30 °C and + 70 °C, as well as the interval of the measurement which is ±2000 W. The other characteristics of HPF01 are: a plate diameter of 80 mm, a plate thickness of 5 mm, and a weight of 200 g without cable.

2.2.2 Experimental Method

In our experimental work, the tested concrete cubes are laterally insulated to ensure a unidirectional heat transfer flow between the two faces of the block at T_1 and T_2, where $T_2 > T_1$ (according to Fourier's law). The following assumptions are considered: No heat generation, permanent regime, constant thermal conductivity and unidirectional conduction. The thermal resistance is determined using Fourier law applied to a unidirectional system in a permanent mode such as:

(a) (b)

Figure 5. Cube 1 without EPS (a) and cubes 2-13 with different percentages and different diameters of EPS beads.

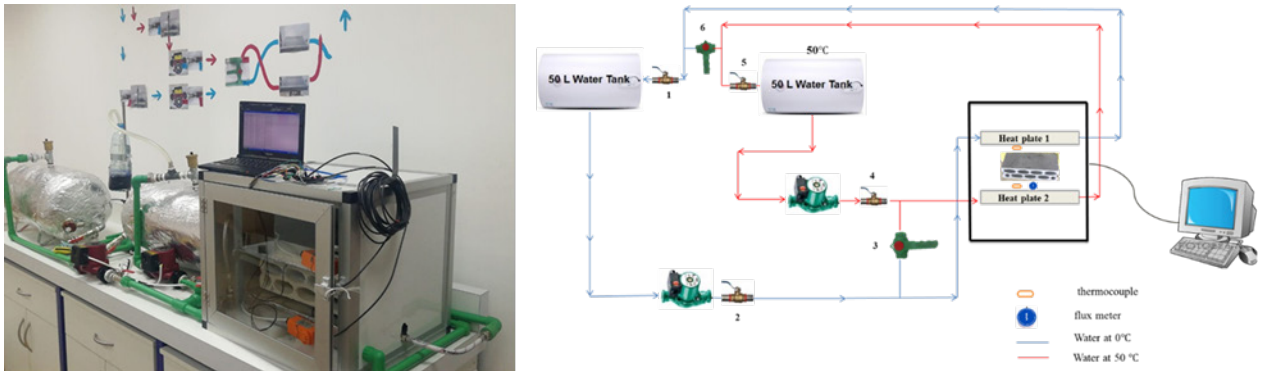

(a) (b)

Figure 6. Photography (a) and schematic representation (b) of the experimental set-up.

$$R = \frac{T1-T2}{\varphi} \quad (3)$$

where R is the thermal resistance of the sample in m^2K/W.

In order to validate the thermal conductivity of cube one without EPS, the last is placed between the hot plate and the cold one. The heat flow and the temperatures on both sides of the sample are recorded using computer software (Arduino). Then, the thermal resistance is found using Equation (3) when the temperature and the heat flow reach their stabilities. After that, the thermal conductivity λ is obtained using the following Fourier's law equation:

$$\lambda = \frac{e}{R} \quad (4)$$

3. Results and Discussion

3.1 Experimental Measurement Results

The block is heated from the bottom side (temperature T_1) until reaching a steady state condition while the second side is kept at ambient temperature conditions. The results show that the steady is reached after about two hours (Figure 7). The hot side temperature T_1 reaches a steady state value of 40.57 °C whereas temperature T_2 slightly increases to reach 30.79 °C. The heat flux reaches a maximum of 420 $W \cdot m^{-2}$ after 18 minutes then starts to decline and stabilizes at a value of 169.57 $W \cdot m^{-2}$.

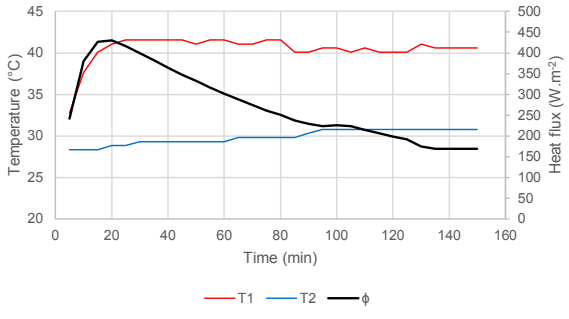

Figure 7. Heat flux and Temperatures variation for C1.

Based on the experimental measurements and Equations (3) and (4) the thermal conductivity can be computed. The measured thermal conductivity was found to be 1.734 $W \cdot m^{-1} \cdot K^{-1}$; this value is in the range of the thermal conductivity values of traditional concrete which can be found in the range of 1.5 $W \cdot m^{-1} \cdot K^{-1}$ to 2 $W \cdot m^{-1} \cdot K^{-1}$. Indeed, the Brazilian association of technical standards [20] stated that the thermal conductivity of concrete with a density between 1600 kgm^{-3} ~ 2100 kgm^{-3} is in the range of 1.40 $W \cdot m^{-1} \cdot K^{-1}$. Similarly, Leiva et al. [21] tested conventional concrete blocks and found that the thermal conductivity is equal to 1.63 $W \cdot m^{-1} \cdot K^{-1}$.

In the same way, the thermal conductivities of samples C2 – C13 were computed and reported in Figure 8.

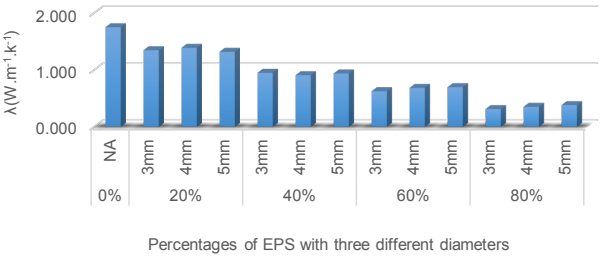

Figure 8. Thermal conductivities for 13 tested specimen.

3.2 Numerical Validation

To validate the experimental measurements concerning numerical models used for concrete mixtures, the experimental results were compared to the Maxwell-Eucken model (MEM) [22] to evaluate the validity of the results. Composite or heterogeneous materials have been extensively used in the applications of heat transfer processes, where thermal conductivity has been hugely affected by its structure as well as its composition. The thermal conductivity of all materials having a simple physical structure can be demonstrated using a prevailing ultimate

structural model. This model is one of the most common models, which is used for all materials with sophisticated physical structures. Equation (5) is the key to proving the effectiveness of our model:

$$\lambda = \lambda_1 \frac{2\lambda_1+\lambda_2-2(\lambda_1-\lambda_2)V_2}{2\lambda_1+\lambda_2+(\lambda_1-\lambda_2)V_2} \quad (5)$$

where λ is the effective thermal conductivity, λ_1 and λ_2 are the thermal conductivities of each phase (concrete and EPS beads respectively), and V_2 is the respective volume fraction of EPS beads.

The EPS beads thermal conductivity was assumed to be equal to 0.04 $W \cdot m^{-1} \cdot K^{-1}$ [23-25].

Table 3 shows the experimental thermal conductivity λ_{Exp} (3 mm) which is compared to the MEM model. The comparison between the experimental results and the MEM model shows very similar results with relative errors of less than 10%.

Table 3. Comparison between our Experimental results and MEM model result.

V_2	λeq,num (MEM)	λExp (3 mm)	Relative Error (%) (2-3 mm)
0.2	1.287	1.345	4.31
0.4	0.900	0.949	5.16
0.6	0.570	0.624	8.65
0.8	0.287	0.311	7.72

3.3 Influence of EPS Diameter on the Thermal Performance of EPS Concrete Mixtures

Figure 9 indicates that for each EPS ratio (20%, 40%, 60% and 80%), the effect of the diameter of the bead (3 mm, 4 mm, 5 mm) on the equivalent thermal conductivity of the concrete sample is very low and the values for the same EPS ratio are in the same range (flat curves). As a result, it can be concluded that the EPS diameter variation has a very slight effect on the thermal conductivity of the EPS concrete mixture.

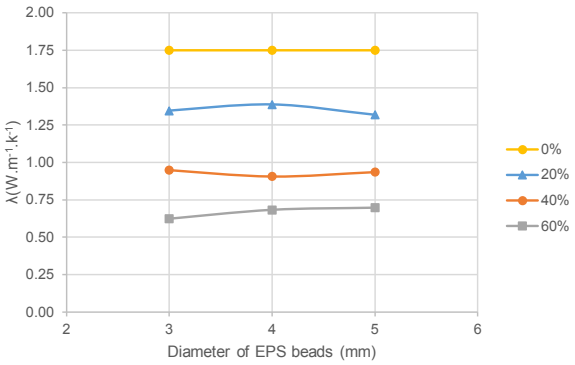

Figure 9. Effect of EPS beads diameter on the thermal conductivity for different volumetric ratios.

3.4 Influence of the EPS Percentage on the Heat Transfer

The analysis of the impact of the EPS ratio on the equivalent thermal conductivity of the EPS concrete mixture clearly shows that the thermal conductivity decreases linearly with the increase of the EPS ratio (Figure 10). The three curves representing the three different studied diameters represent the same decreasing shape. The equivalent thermal conductivity decreases by 0.18 $W \cdot m^{-1} \cdot K^{-1}$ (around 10%) for each 10% of EPS beads replacement.

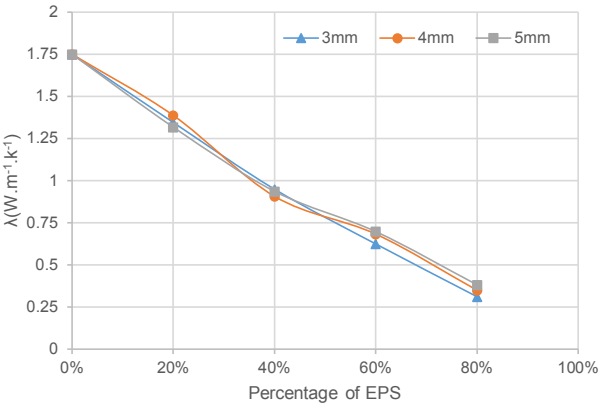

Figure 10. Effect of the volumetric ratio on the thermal conductivity for different EPS beads diameters.

4. Economic and Environmental Impact

One of the major benefits of adding recycled aggregates to construction materials is to reduce their environmental impact and their manufacturing cost. It is thus interesting to assess and compare the benefits of incorporating EPS beads in the hollow blocks concrete mixture on their cost and the environmental benefits of this substitution.

The aim of the economic study is to display in detail all the required materials used during the experimental laboratory work as well as their prices in US$ in order to evaluate the financial impact of this substitution.

One of the main important factors that influence the cost analysis is the price of the EPS beads. The beads can be bought from the market in bags but they are relatively expensive (around 0.5 US$/kg), especially when dealing with large amounts such as building applications. It is thus more relevant to use other resources for EPS beads at a more affordable price. In this case study a 2 kW shredder is used capable of delivering two cubic meters per hour (Figure 11).

The cost of bulk polystyrene wastes is assumed to be 0.05 US$/kg, and the electricity cost is assumed to be 0.15 US$/kWh. Based on these assumptions, to be able to produce one cubic meter of polystyrene (35 kg), the elec-

tric energy needed is 1 kWh and the cost of needed bulk wastes is 1.75 US$. The total cost of one cubic meter of shredded EPS beads is thus around 2 US$ including the manpower cost.

Figure 11. Example of EPS shredder.

Table 4 summarizes the unit costs of the different ingredients used in the preparation of the EPS concrete mixture.

Table 4. Unit prices of the used materials.

Material	Cost (US$)
1 cubic meters of EPS	2
1 ton of cement	110
1 ton of sand and gravel	10
1 cubic meters of water	2

In what follows, the cost comparison will be based on the samples C1 – C5 where C1 represents the sample without any EPS content and C2, C3, C4, and C5 represent the samples with 2 mm EPS beads with 20%, 40%, 60%, and 80% volumetric ratios respectively.

Based on the above assumptions, the mixture content and prices of the EPS concrete mixtures are reported in Table 5.

Table 5. Estimated cost of one cubic meter of EPS concrete for samples C1, C2, C3, C4, and C5.

Sample	C1	C2 (20%)	C3 (40%)	C4 (60%)	C5 (80%)
EPS (kg)	0	7	14	21	28
EPS (US$)	0	0.4	0.8	1.2	1.6
Cement (kg)	350	350	350	350	350
Cement (US$)	38.5	38.5	38.5	38.5	38.5
Water (kg)	300	300	290	280	270
Water (US$)	0.6	0.6	0.58	0.56	0.54
Coarse and fine aggregates (kg)	1750	1575	1400	1225	1050
Coarse and fine aggregates (US$)	17.5	15.75	14	12.25	10.5
Total cost (US$)	56.6	55.25	53.88	52.51	51.14

The results of the economic analysis show that the use of recycled EPS as replacement for stone aggregates not only improves the thermal insulation of the concrete elements, but also reduces the cost of the concrete by up to 10% for 80% of EPS replacement.

Furthermore, the analysis also shows that the maximum price of EPS that does not induce a raise in the concrete cost is 9 US$. Above this value the price of EPS concrete will start to be greater than the normal concrete (C1).

On the other hand, the use of EPS concrete mixture also saves EPS wastes to be dumped in landfills especially that these wastes are not recyclable and they require a large volume due to their very low density. The use of 1 cubic meter of sample C5 (80% EPS ratio) can thus save 800 liters of EPS to be dumped and will also save the excavation of 800 liters of rocky soil.

5. Conclusions

In order to enhance the thermal properties of concrete building materials, insulating aggregates can be incorporated into the composition of concrete mixtures. One of these potential materials is the EPS (Expanded Polystyrene) beads. Due to the massive production of EPS, huge quantities are treated as material waste despite their importance in terms of thermal insulation applications. Three different diameters of EPS (3 mm, 4 mm and 5 mm) were used with different percentages (20%, 40%, 60% and 80%) in order to investigate the effect of EPS on the thermal properties of concrete. The results showed that the percentage of incorporated EPS reduces the thermal conductivity linearly with a rate of 10% decrease in thermal conductivity for every 10% increase in EPS volumetric ratio. On the other hand, the EPS beads' diameters have a negligible impact on the thermal performance of the concrete tested samples.

This work delivers valuable data to enhance the understanding of the thermal properties of a mixture by underlining the effect of the aggregate size and ratio on the thermal performance of concrete cubes. It also provides a better understanding of the thermal influence of aggregates on concrete mixtures, which should be addressed in order to determine the ideal cement/aggregate proportions to evaluate the ratio of solid waste leading to the greatest thermal physical properties. The economic analysis also highlighted the cost and environmental benefits of using recycled wastes in concrete mixtures. The use of EPS as a substitution for concrete aggregates in construction applications would thus reduce the number of materials sent to landfill, and preserve natural materials for future use by improving the thermal performance of the building through its low thermal conductivity.

The main limitation of this paper is that it does not analyze the shredded polystyrene shapes and their impact on the thermal properties of the resulting mixture but rather assumes that the obtained aggregates are perfectly spherical; this factor will be addressed in future research works by comparing manufactured EPS beads through the pre-expansion process with recycled EPS aggregates.

Conflict of Interest

The authors have no conflicts of interest to declare. All co-authors have seen and agree with the contents of the manuscript.

References

[1] International Energy Agency, 2013. Transition to Sustainable Buildings.

[2] Sassine, E., Cherif, Y., Dgheim, J., et al., 2020. Investigation of the mechanical and thermal performances of concrete hollow blocks. SN Applied Sciences. 2. DOI: https://doi.org/10.1007/s42452-020-03881-x

[3] Yang, J., Du, Q., Bao, Y.W., 2011. Concrete with recycled concrete aggregate and crushed clay bricks. Construction and Building Materials. 25, 1935-1945.

[4] Medina, C., De Rojas, M.S., Frías, M., 2012. Reuse of sanitary ceramic wastes as coarse aggregate in ecoefficient concretes. Cement & Concrete Composites. 34, 48-54.

[5] Yoshida, A., Terazono, A., Ballesteros, F.C., et al., 2016. Ewaste recycling processes in Indonesia, the Philippines, and Vietnam: A case study of cathode ray tube TVs and monitors. Resources Conservation & Recycling. 106, 48-58.

[6] Zhang, G.H., Zhu, J.F., Okuwaki, A., 2007. Prospect and current status of recycling waste plastics and technology for converting them into oil in China. Resources Conservation & Recycling. 50, 231-239.

[7] Mohammed, B., Hossain, K.M.A., Swee, J.T.E., et al., 2011. Properties of crumb rubber hollow concrete block. Journal of Cleaner Production. 23, 57-67. DOI: https://doi.org/10.1016/j.jclepro.2011 .10.035

[8] Chen, B., Liu, J., 2004. Properties of lightweight expanded polystyrene concrete reinforced with steel fiber. Cement and Concrete Research. 34, 1259-1263.

[9] Khatib, J.M., Herki, B.A., Kenai, S., 2013. Capillarity of concrete incorporating waste foundry sand. Construction and Building Materials. 47, 867-871.

[10] Bhutta, M.A.R., Ohama, Y., Tsuruta, K., 2011. Strength Properties of Polymer Mortar Panels Using Methyl Methacrylate Solution of Waste Expanded Polystyrene as Binder. Construction and Building Materials. 25, 779-784.

[11] Khatib, J.M., Herki, B.A., Elkordi, A., 2019. Characteristics of concrete containing EPS. Use of Recycled Plastics in Eco-efficient Concrete. 137-165.

[12] Sassine, E., Cherif, Y., Dgheim, J., et al., 2020. Experimental and Numerical Thermal Assessment of EPS Concrete Hollow Blocks in Lebanon. Journal of Materials in Civil Engineering. 32, 41-47.

[13] Ganesh Babu, K., SaradhiBabu, D., 2004. Performance of fly ash concretes containing lightweight EPS aggregates. Cement and Concrete Composites. 26, 605-611.

[14] Sayadi, A., Tapia, J.V., Neitzert, T.R., et al., 2016. Effects of expanded polystyrene (EPS) particles on fire resistance, thermal conductivity and compressive strength of foamed concrete. Construction & Building Materials. 112, 716-724. DOI: https://doi.org/10.1016/j.conbuildmat.2016 .02.218

[15] Karade, S.R., 2010. Cement-bonded composites from lignocellulosic wastes. Construction & Building Materials. 24, 1323-1330.

[16] Xuan, D.X., Poon, C.S., Zheng, W., 2018. Management and sustainable utilization of processing wastes from ready-mixed concrete plants in construction: a review. Resources Conservation & Recycling. 136, 238-247.

[17] Mohammed, B.S., Hossain, K.M.A., Swee, J.T.E., et al., 2012. Properties of crumb rubber hollow concrete block. Journal of Cleaner Production. 23, 57-67.

[18] Ling, T.C., Poon, C.S., Wong, H.W., 2013. Management and recycling of waste glass in concrete products: Current situations in Hong Kong. Resources Conservation & Recycling. 70, 25-31.

[19] AFNOR-NF EN 12939, 2021. Thermal performance of building materials and products—Determination of thermal resistance by means of guarded hot plate and heat flow meter methods—Thick products of high and medium thermal resistance.

[20] Brazilian association of technical standards (ABNT), 2003. NBR 15220: Thermal performance in buildings—Part 1, 2, 3 and 4. Rio de Janeiro.

[21] Leiva, C., Solís-guzmán. J., Marrero, M., et al., 2013. Recycled blocks with improved sound and fire insulation containing construction and demolition waste. Waste Management. 33, 663-671.

[22] Wang, J., Carson, J.K., North, M.F., et al., 2008. A new structural model of effective thermal conductivity for heterogeneous materials with co-continuous phases. International Journal of Heat & Mass Transfer. 51, 2389-2397. DOI: https://doi.org/10.1016/j.ijheatmasstransfer.2007.08.028

[23] Dixit, A., Pang, S.D., Kang, S.H., et al., 2019. Lightweight structural cement composites with expanded polystyrene (EPS) for enhanced thermal insulation. Cement and Concrete Composites. 102, 185-197. DOI: https://doi.org/10.1016/j.cemconcomp.2019.04.023

[24] De Moraes, E.G., Sangiacomo, L., Stochero, N.P., et al., 2019. Innovative thermal and acoustic insulation foam by using recycled ceramic shell and expandable styrofoam (EPS) wastes. Waste Management. 89, 336-344.

[25] Gnip, I.Ya., Vėjelis, S., Vaitkus, S., 2012. Thermal conductivity of expanded polystyrene (EPS) at 10 °C and its conversion to temperatures within interval from 0 to 50°C. Energy and Buildings. 52, 107-111.

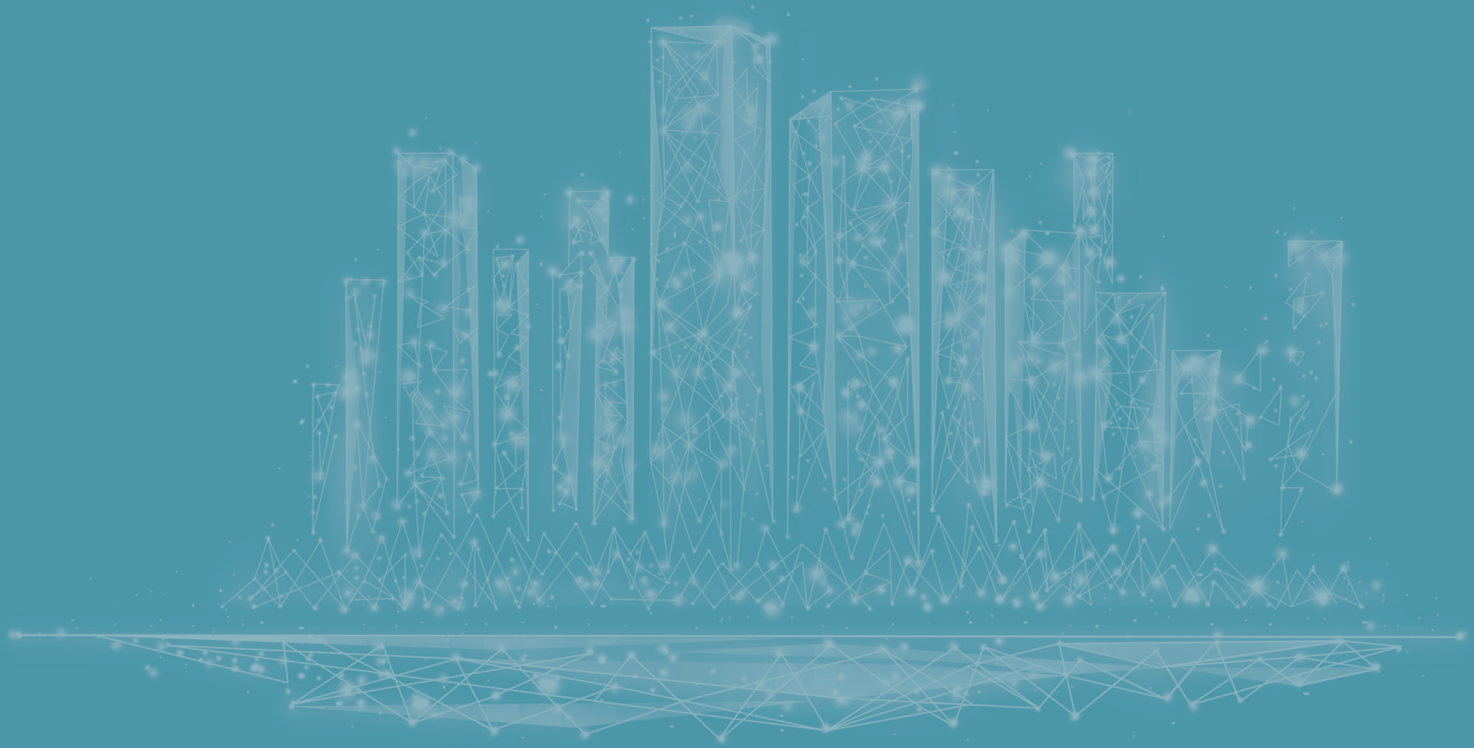

BILINGUAL
PUBLISHING CO.
Pioneer of Global Academics Since 1984

Tel:+65 65881289
E-mail: contact@bilpublishing.com
Website:ojs.bilpublishing.com

2630-5216
02
9 772630 521224